Karlsruher Institut für Technologie

Master Thesis

Assessment of sediment and nutrient fluxes from discharge measurements by means of Large Volume Sampling and other quantification approaches for the Kraichbach catchment

Institut für Wasser und Gewässerentwicklung
Bereich Siedlungswasserwirtschaft und Wassergütewirtschaft

Submitted by:	Mingjiao Zheng
Matric number:	2082397
Supervisors:	PD Dr.-Ing. Stephan Fuchs
	Dr.-Ing. Geoökol. Stephan Hilgert
	M.Sc. Adrian Wagner

Submission date: 14th December, 2018

Declaration of Authorship

I hereby declare that the thesis submitted is my own unaided work. All direct or indirect sources used are acknowledged as references. Furthermore, I agree that my thesis may be placed in the library of the Institute for Water and River Basin Management, Department of Aquatic Environmental Engineering and may be reproduced for research and teaching purposes.

_____ _____

Site, Date Signature

Abstract

Although being natural and essential components of the aquatic environment, sediment and nutrients (nitrogen and phosphorus) with elevated levels can be problematic to receiving ecosystems. Hence, an accurate quantification of their fluvial concentrations and budgets is significant for an integrated watershed management. In a conventional way, concentration variations are traced through manual collection and laboratory analysis of samples, which in combination with continuous flow rate monitoring can result in pollutant loads. However, it is not only time-consuming and labor-intensive but also likely to bring about extensive uncertainties and bias. In this context, for the Kraichbach catchment in Baden-Württemberg (Germany), more reliable estimation approaches were investigated at different timescales in this thesis.

On the foundation of measurements from a Large Volume Sampler (LVS) located at Ubstadt Gauge and continuous flow rate records, 18 rating curves and two sub-methods, Time-split and Volume-split, were developed and assessed. Exponential rating curves were proved to be optimal for particulate matters including total suspended solids (TSS), particulate nitrogen (N_part), particulate phosphorus (P_part) and total phosphorus (TP), while the relationships between dissolved (N_dis) or total nitrogen (TN) and discharges were more appropriately described by linear regression models. As for methods, T-split exhibited the equal capability of N_dis and TN budgeting to V-split, but it constantly underestimated in dry years in the meantime grossly overpredicted in wet years. In addition, constitution analysis showed that, by means of either method, the highest 20% discharge percentile accounted for averagely 88% of total transportable sediments. Therefore, it can be confirmed that only occasionally occurring flood events were the most decisive contributor to fluvial sediment yield. Furthermore, notable correlations were found to exist among those annual yields of parameters of interest, which provided another potential way to budget anyone of them from others under data-constrained circumstances.

In comparison to LVS-based models, the turbidity-based approach suffered from great underestimation (40%-329%) in most of our cases. Hilden approach estimated up to 200%-300% fewer budgets of nutrients and sediment in 2017/2018, during which grab samples were mostly collected during low flow conditions. As a result, neither of them was decided to be reliable for the Kraichbach watershed. However, an adjusted version of Hilden approach generated accurate budgets, since it was calibrated by LVS-based results and emphasized the importance of peak events for budgeting.

Keywords: the Kraichbach catchment, Large Volume Sampler, load estimation

Table of contents

List of tables

List of figures

List of abbreviations

AD	Atmospheric deposition
COD	Chemical Oxygen Demand
CSO	Combined Sewer Overflow
DCS	Decentralized household systems
DO	Dissolved Oxygen
DOC	Dissolved Organic Carbon
EPA	Environmental Protection Agency
Er	Erosion
EU	The European Union
GW	Groundwater
HQ_T	T- jährlicher Hochwasserabfluss (high flow in T years)
ID	Industrial Discharges from factories
IF	Interflow at upper groundwater
IQR	Interquartile Ranges
LUBW	Landesanstalt für Umwelt, Messungen und Naturschutz Baden-Württemberg
LVS	Large Volume Sampler
MCLG	Maximum Contaminant Level Goals
MHQ	Mittlerer Hochwasserabfluss (mean high flow)
MNQ	Mittlerer Niedrigwasserabfluss (mean low flow)
MoRE	Modeling of Regionalized Emissions
MQ	Mittlere Abfluss (mean flow)
MSFD	Marine Strategy Framework Directive
N_2	Nitrogen gas
NH_4-N	Ammonia nitrogen
NO_2-N	Nitrite nitrogen
NO_3-N	Nitrate nitrogen
N_dis	Dissolved nitrogen
N_part	Particulate nitrogen
P_dis	Dissolved phosphorus
P_part	Particulate phosphorus
PO_4-P	Phosphate phosphorus
Qmax_h	Hourly maximum discharge
R^2	Coefficient of determination

RMSE	Root Mean Square Error
RMSE*	Normalized Root Mean Square Error
RSD	Relative Standard Deviation
SR	Surface Runoff from arable land and pastures
SSC	Suspended Solids Concentration
SSO	Separate Sewer Overflow
SSR	Residual Sum of Squares
SST	Total Sum of Squares
STD	Standard Deviation
T-split	Time-split method
TD	Tile Drainage of agricultural land
TN	Total Nitrogen
TP	Total Phosphorus
TSI	Trophic State Index
TSS	Total Suspended Solids
US	Urban Systems
V-split	Volume-split method
WFD	Water Framework Directive
WWTP	Waste Water Treatment Plant

1. Introduction

1.1. Motivation

Since the 1970s, an accurate quantification of the fluvial budgets of sediment and sediment-associated chemicals has gained continuously increasing interest (Horowitz et al. 2015, p. 531). In spite of the indispensable role of sediment played in shaping the landscape, forming ecological habitats and delivering nutrients, it generates plenty of problems (Vercruysse et al. 2017, p. 39). In many areas of the world, elevated concentrations of sediment along with relevant contaminants and nutrients have been identified to substantially account for the impaired aquatic environment (Evans-White et al. 2013, p. 1002), triggering water quality deterioration, reservoir sedimentation, channel and harbor silting, infrastructure damage as well as ecological communities and recreational values degradation (Sadeghi et al. 2008, p. 198).

In recognition of aforecited multi-dimensional negative effects regarding suspended sediments, many studies have been conducted for the purpose of aquatic ecosystems restoration and human health protection (Owens et al. 2005, p. 19). Various techniques have been proposed such as soil erosion control measures, massive afforestation, land use alteration, sediment management, last but not least, operational improvements on water supply and sewerage treatment infrastructures until the water quality complies with permits and standards. National, federal and local organizations have also made great efforts e.g. remediation plans for extant fluvial pollution, implementation of relevant policies to tackle these issues (Mueller and Helsel 1999a).

However, despite decades of studies, the prevalence of potamic sediment and nutrients still remains not fully under control (Vercruysse et al. 2017, p. 39). To guide water-resource researchers and policymakers to make wise decisions (Mueller and Helsel 1999a) and assess the efficacy of protective measures, a thorough understanding of pollutant sources and pathways (Vercruysse et al. 2017, p. 38), precise quantification of their concentrations and loads within the catchment of interest, and reliable analysis of the content variability at different temporal and spatial scales are necessary for an integrated watershed management (Girolamo et al. 2015, p. 136; Fox et al. 2016b, p. 603).

1.2. Study catchment description

Land use is a determinant factor of watershed sediment pollution (Liu et al. 2017, p. 639). An accelerated erosion rate usually relates to the clearance of vegetation coverage and arable land expansion (Fox et al. 2016b, p. 609). Anthropogenic activities in surrounding residential areas can also encourage the entry of contaminants into waterways. Therefore, the land use and other characteristics of Kraichbach watershed need to be elaborated prior to analysis.

The Kraichbach (also named Kraich) is an approximate 55 km long river located in northwest Baden-Württemberg. It originates from the Kraichgau district near the southern municipality of Sternenfels, Enzkreis to be specific. The stream then flows to the northwest across Oberderdingen, Flehingen, Gochsheim, Münzesheim, Unteröwisheim, Ubstadt, Bad Langenbrücken and Kronau, all in the district of Karlsruhe. It then enters the region of Rhein-Neckar-Kreis and flows through Sankt Leon, Reilingen, Hockenheim before converging into Altrhein at Ketsch (Wikipedia 2018).
The catchment area until Ubstadt in all is roughly 160 km². The largest percentage of the area is occupied by agricultural land, accounting for nearly half of this region. However, only half of the arable lands actually contribute to the fluvial sediments, that is 39 km², to be precise (GALF 2018). One-fifth of the catchment comprises of forests, including broad-leafed, coniferous and mixed forests. Next comes sparse trees, whose percentage is slightly higher than that of residential housing. Falling behind the former items, wetland, water surface, sealed surface, and bare soil constitute the lowest proportions, each less than 0.1%.
Moreover, Landwirtschaftliches Technologiezentrum Augustenberg has announced a weighted topsoil total phosphorus mean concentration in arable lands within this catchment during the years 1995-2012, that was 1.02 g/kg (LTZA 2018), and the mean annual sediment input from agriculture was 938.5 t/a (GALF 2018).

Figure 1.1 illustrates where the wastewater treatment plants (WWTP), data loggers, gauge station and Large Volume Sampler (LVS) are located. Loggers record turbidity, dissolved oxygen (DO) and temperature values every ten minutes. Discharge data are detected at a time interval of 15 minutes at Ubstadt Gauge, where the LVS performs. One of the WWTP is situated nearby the gauge, whose measurements to a certain extent get affected.

1.3. Objectives of the thesis

The quality of rivers and involved watersheds are more than ever in need of precise control. Therefore, a need has developed for reliable techniques to estimate fluvial sediment and nutrient budgets. In this thesis, an accurate load estimation for the Kraichbach catchment at different temporal scales is the priority task. On the basis of LVS measurements, rating curves between hourly maximum discharges and the mean concentrations of TSS, nitrogen species (total/dissolved/particulate) and phosphorous species (total/particulate) during the sampling periods are required to be developed. In the meantime, a simple scaling mass balance by means of Hilden approach is accomplished as a common reference.

Additionally, a site-specific regression model between in-situ measured turbidity values and suspended sediment concentrations (SSC) is expected to be established, aiming to predict SSC and thereby computing the sediment budget for a defined timescale.
The intra-comparison of the outcomes from diverse budgeting approaches and inter-comparison of them with a pollutant input model MoRE are also of importance for further applications after the discussion of probable error sources.
Furthermore, the contribution of peak events is investigated.
Ultimately, on the foundation of overall results, one can discuss different pollutant sources, ecological and economic consequences and feasible watershed management measures.

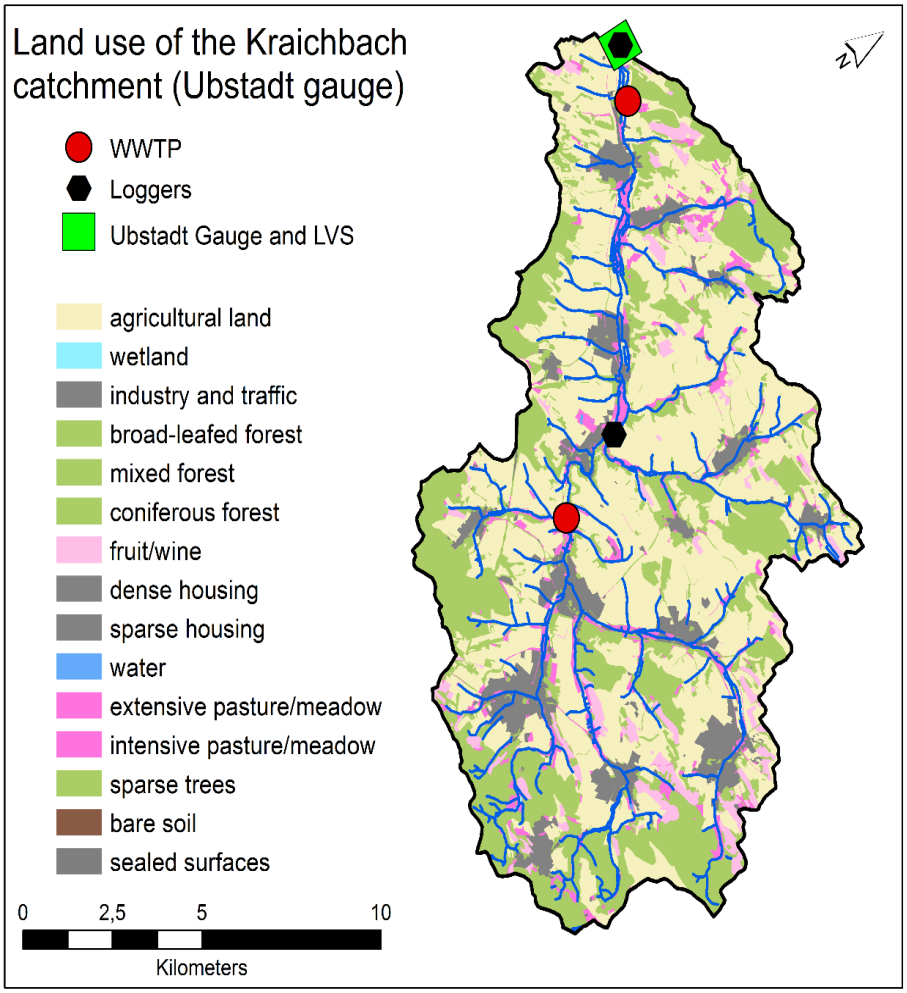

Figure 1.1 Land use and monitoring stations in the Kraichbach catchment (IWG-SWW 2018)

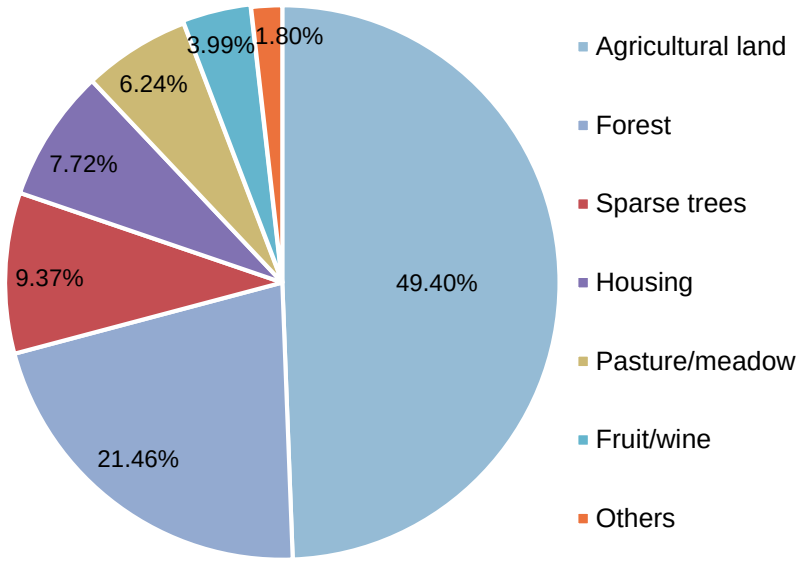

Figure 1.2 Land use percentages in the Kraichbach catchment. Others: industry and traffic (1.64%), wetlands (0.06%), water (0.05%), sealed surface (0.04%), bare soil (0.02%) (source of data: IWG-SWW 2018).

2. Background

2.1. Review of method development

The past few decades have witnessed a rapid development of approaches to estimate sediment and associated nutrient concentrations and thereby yields in fluvial systems. These include manual collection and analysis of samples, empirical rating curves construction, surrogates e.g. turbidity regression model development and remote sensing techniques application.

2.1.1. Traditional manual sampling method

The determination of loads entails paired flow rates and concentration data (Horowitz et al. 2015, p. 531). Flow rates usually are accurately and continuously monitored, whereas adequate concentration analysis can be a challenge.

Conventionally, concentration variations are provided by manually grabbed samples from the field at defined time intervals and then measured in the laboratory. On the one hand**,** normative laboratory measurement offers high accuracy (Gholizadeh et al. 2016). On the other hand, it can be inappropriate and questionable. Foremost, the frequent collection and analysis of samples are time-consuming, labor-demanding and costly (Gholizadeh et al. 2016) and it suffers from random operational errors and water quality degradation problems during preservation (Kulasova et al. 2012b, p. 2). Under such circumstances, a discrete sampling campaign is preferable (Stevens and Smith 1978,

p. 829). However, risks have still been run when infrequent sampling regime fails to capture storm events (Lannergård et al. 2018, p. 104), which occasionally occur however can dominate annual pollutant loads. In this case, sediment and nutrient yields will experience gross underestimation (Kulasova et al. 2012a, p. 1) and their temporal variations become more out of reach.
In this section, a traditional discharge-corrected standard method after Hilden (2003) (in the following called Hilden approach) will be explained.

1) Definition of annual load

Quoting from Hilden, the annual load is defined as the number of substances transported through a river's cross section within a certain year. When the measured concentration is viewed to be on behalf of the entire cross-section, the transport T, as the product of discharge and concentration, comes into being (Hilden 2003, p. 6, transl.: M.Z.).

$$T(t) = \frac{1}{1000} * Q(t) * c(t)$$

(Equation 1) (Hilden 2003, p.6)

Where Q is the discharge (m^3/s); c is the concentration (ug/L or mg/L), depending on time t. The unit of measurement for transport T is usually g/s or kg/s.
The standard annual load F (kg or t) is the sum, namely the integral of delivered mass throughout a whole year of measurement (Hilden 2003, p. 6, transl.: M.Z.).

$$F = \frac{1}{1000} * \int T(t)\,dt = \frac{1}{1000 * 1000} * \int Q(t) * c(t)\,dt$$

(Equation 2) (Hilden 2003, p.6)

2) Data basis

Point discharge and water quality parameter concentration, as described before, hypothetically represent for the whole cross-section, which undoubtedly induces statistical and systematical errors to mass balance. Moreover, their out-of-sync detection schedules can harm the validity of results. Explicitly, due to human labor, financial and technical restraint, frequent concentration measurement is unrealistic, while continuous discharge recording by automated probes is achievable in most cases (Hilden 2003, p. 8, transl.: M.Z.).
Two kinds of sampling were itemized by Hilden, i.e. single and mixed sampling. The former refers to the collection of samples at regular time intervals and ideally, the subsequent analysis is as immediate as possible. In water science practice, the single sample represents the water body status in the specific sampling interval and location. Whereas mixed sampling is equipped with automatic sampling devices, which take in a fixed volume of water every time at a short interval (e.g. hourly) and accumulate for a

definite period (e.g. two weeks), thus producing a mixed sample, whose concentration is assumed to be the mean concentration during the period (Hilden 2003, p. 9, transl.: M.Z.).

The question lies in at what sampling frequency is the true concentration measured. Typically, a sampling frequency of once every 15 minutes is satisfactory. However, it is not practical, especially in the long term due to the massive time and human labor required (Harrington and Harrington 2013, p. 27). By Hilden, sampling interval is one, two, or four weeks, which gives 52, 26, or 13 samples with single or mixed mean concentrations in a measurement year (Hilden 2003, p. 9, transl.: M.Z.).

3) Modified method

Standard method expresses the annual load as Equation 3.

$$\overline{F} = \frac{365 * 86400}{1000 * 1000} * \frac{1}{N} * \sum_{i=1}^{N} c(t_i) * Q(t_i)$$

(Equation 3) (Hilden 2003, p.10)

Where $\overline{F}$ is the standard annual load (t); N is the sampling time; c (mg/s) and Q (m^3/s) are the concentration/flux and discharge value at sampling time point t_i respectively.

Apparently, the likelihood that a wide range of single samples are coincidentally collected during relatively high or low conditions brings about over- or underestimation issues (Hilden 2003, p. 12, transl.: M.Z.). This possible bias promotes the modified version of Hilden method, which introduces a correction factor, the ratio of mean annual discharge $\overline{Q}$ (m^3/s) and mean sampling discharge Q_M (m^3/s).

$$\overline{Q} = \frac{1}{365} * \sum_{j=1}^{365} Q_j$$

(Equation 4) (Hilden 2003, p.12)

$$Q_M = \frac{1}{N} * \sum_{i=1}^{N} Q_i$$

(Equation 5) (Hilden 2003, p.12)

Modified annual load F_Q (tonne) is then adjusted on the basis of the standard annual load $\overline{F}$ with a reduced impact from non-representative sampling in a dynamic flow regime (Hilden 2003, p. 12, transl.: M.Z.).

$$F_Q = \overline{F} * \frac{\overline{Q}}{Q_M}$$

(Equation 6) (Hilden 2003, p.12)

2.1.2. New techniques

1) Flow-concentration rating curves

Over a long time, discharge or water level is viewed as an indicator of mean sediment load (Vercruysse et al. 2017, p. 45), so the establishment of flow-concentration rating curves for a specific location is one of the most widely used approaches for estimation (Yang and Lee 2018, p. 171). A rating curve is normally developed based on continuous time series of flow rates and limited manual concentration measurements (Atieh et al. 2015, p. 1095), commonly expressed as a power or log-log function (Yang and Lee 2018, p. 171). Though questions have been raised about the accuracy of sediment rating curve since it presents a high degree of scattering and hysteresis, tending to underpredict high, and overpredict low SSCs (Horowitz 2003). This means the regression curve might be biased because it has the tendency to overlook fairly important discharge outliers (Vercruysse et al. 2017, p. 42). But the advantages of the rating curve method are also appealing: i) it is simple to construct since discrete and relatively small datasets are required (Vercruysse et al. 2017, p. 42); ii) long-term SSC and fluxes are predictable by only streamflow data once the relation model is established (Girolamo et al. 2015, p. 142); iii) quick and inexpensive operation makes it a competitive choice.

To date, there has been a wide agreement on the overwhelming contribution of a small number of flood events caused by heavy rainfall or snowmelt to fluvial sediment transport (Vercruysse et al. 2017, p. 40). Nutrient contents in the river can also be subject to flushing or dilution during storms. While base flows, for most rivers, are more ubiquitous but bring a much smaller proportion of the total annual SS. As a result of all the foregoing considerations, it is realized that the sampling campaign including frequency, number and scheduling (Quilbé et al. 2006) can exert great influence on the estimates of SSC and load (Horowitz et al. 2015, p. 533), accordingly deserves special attention (Walling 2006, p. 196). Kulasova et al. (2012) found that a better level of precision and accuracy was achieved when sampling on times of peak flows. Stevens and Smith (1978) reported that sampling was supposed to be flow-proportional (Rekolainen et al. 1991) rather than on a rigid protocol. Horowitz et al. (2014) concluded that hydrology-based, as opposed to calendar-based sampling, was in either case the most advisable regime, and suggested that the collection of samples should cover as broad a range (at least 80%) of annual flow rates as possible. Besides, full-daily sampling and stratified sampling were suggested by Johnes (2007) to achieve a more reliable performance.

The analysis of environmental samples instantly after collection is a general consensus. However, logistic constraints make it frequently essential to store them before processing (Sara Bogialli et al. 2014, p. 287). To avoid degradation or contamination during transportation and storage, and so as to achieve minimal invariability of sample

characteristics, pre-treatments are every now and then conducted. The most common preservation methods are limited to acidification, chemical addition, refrigeration, and minimal exposure to the light (Sara Bogialli et al. 2014, p. 288). Particular attention needs to be devoted to sample containers, specific conditioning or cleaning may be required in advance of use.

2) Surrogates techniques

Recent researches have highlighted the applicability of in-situ surrogates such as turbidity, acoustic signals and satellite remote sensing spectra (Horowitz et al. 2015, p. 532; Rymszewicz et al. 2017, p. 100) to generate continuous SSCs. Although the capability and convenience of surrogate regression models to evaluate water quality are undeniable, these techniques are faced with limitations. First, in most cases, surrogate parameter detection devices merely reveal individual point situation rather than depth-integrated and cross-sectionally representative information (Horowitz et al. 2015, p. 532). Second, they are not sufficiently precise so as to eliminate the need for traditional sampling analysis since site-specific calibration is indispensable (Gholizadeh et al. 2016). Nevertheless, detecting water turbidity as a proxy for SSC using turbidimeter or nephelometer is especially widely received and well-established in freshwater systems.

In 2014, Rügner et al. published a paper in which they described that an accurate assessment of particle concentration dynamics would be achieved by online turbidity sensors based on the investigation of River Neckar and its three contrasting sub-catchments (Ammer, Goldersbach, Steinlach) in Southwest Germany (Rügner et al. 2014, p. 197). Surveys such as that conducted by Voichick et al. have shown that a linear increase in turbidity can result from an upsurge in SSC in rivers where the physical properties of SS are limitedly varied (Voichick et al. 2018, p. 1767). Lannergård et al. proved the practicality of high-frequency field detection of turbidity (10-15 minutes) as a proxy for TSS and TP concentrations in a mixed land use catchment in central Sweden (Lannergård et al. 2018, p. 103).

In this context, it is convincing to adopt turbidity discreetly to determine fluvial SSC (Gholizadeh et al. 2016) and, for some simple contexts, particle size distribution (Lawler 2014). Further SSC can be deduced according to a linear relationship between the results from the field turbidity logger and the measured SSCs from manually collected samples (Harrington and Harrington 2013, p. 30). More specific, Rügner et al. have stated that robust and reasonable linear relationships of turbidity [NTU] and SSC (mg/L) in Southern Germany were typically with slopes approximately in the range of 0.9-2.4 (Rügner et al. 2014, p. 192).

This universality of the linear relation has also been challenged by Voichick et al. After examining the collected data from both Colorado River in the US and a laboratory

experiment, they demonstrated that when turbidity exceeded the upper limit of sensors, rising SSC (and accordingly rising turbidity) may result in declining “untrue” turbidity records that appeared to be within the valid measurement range of the optical probes, (Voichick et al. 2018, p. 1767). Additionally, even if surrogate optical devices may be relatively inexpensive to obtain, simple to operate both in laboratory and field, calibration and maintenance effort can be large. And the interrelationships and results tend to be dynamic rather than stable (Horowitz et al. 2015, p. 532). Other than those, the fact that turbidity is as well a function of particle size, shape, and refractive index which however remain non-influential to SSC introduces more uncertainties to this surrogate approach (Berry et al. 2003, p. 10).

2.1.3. Emission model MoRE

In the Federal Republic of Germany, MoRE (Modelling of Regionalized Emissions) system was deployed to annually simulate the pathway-specific substance emissions into rivers on the scale of catchments or sub-catchments (Fuchs et al. 2017). Currently, the annual inputs of nutrients, certain heavy metals, micropollutants, pharmaceuticals, industrial chemicals, biocide, herbicide are quantified (Fuchs et al. 2017). With MoRE, strategies and investments to diminish pollutant releases can be more sophisticated and targeted. However, MoRE results are only a comparison but not validation for modeled budgets, and one needs to be aware of uncertainties of both approaches (Fuchs et al. 2017).

2.2. Parameters

2.2.1. Total suspended solids (TSS)

As a natural part of river systems, TSS represents the entire quantity of organic and inorganic particles dispersed within the water column (Vercruysse et al. 2017, p. 39). It is the portion of total solids retained by a filter (commonly with a pore size of 0.45 µm) from a sample with a known volume and usually measured as the dry weight of the material residue left in the vessel after evaporation and subsequent drying in an oven at a specific temperature (American Public Health Association 1998, p. 215). Relative to bedload, it is the dominant part of sediments emerged in watersheds (Vercruysse et al. 2017, p. 40) and earns more attention.

In natural or background amount, TSS is essential to the ecological function of water bodies (US EPA 2003, p. 9) by constructing landscapes, providing ecological habitats and (Bridge 2003, p. 1) delivering nutrients. But ascending concentration can be problematic for stream balance and aquatic life. High TSS prohibits sunlight from penetrating through the water column and reaching submerged plants, which slows down photosynthesis (Berry et al. 2003, p. 13) thereby leading to losses of certain

macrophytes species (Best et al. 2001) and reducing oxygen production. Increased water temperature due to more heat absorption by sediments and more intensive oxidation processes induced by more particles further result in a lower level of DO (Murphy 2007c). Some fishes as well as pelagic and benthic invertebrates experience population decline and habitat destruction attributed to high sediment concentrations, in the way of abrasion, clogging and interfering with ingestion and respiration organs, reducing growth rates and increasing their vulnerabilities to diseases (Murphy 2007c), and in extreme cases suffocating and burial resulting in mortality (Berry et al. 2003, p. 11). Meanwhile, TSS plays a decisive role in the biological and geochemical cycling of trace elements and nutrients in aquatic systems (Horowitz 2008). The active component of TSS, fine-grained sediments such as silts and clays are particularly be to blame for the transport, storage and release of numerous contaminants and nutrients, including dioxins, radionuclides, heavy and trace metals, pesticides, particulate carbon, phosphorus and nitrogen (Owens et al. 2005, p. 3), by which the ecological state of freshwater and coastal marine environments can be greatly influenced.

To improve our knowledge about long-term TSS dynamics and associated impacts on the geomorphology, ecology and infrastructure, unraveling the driving forces that control TSS level and the interaction of multiple determinants are essential (Vercruysse et al. 2017, pp. 47–48). The occurrence of episodic precipitation or snowmelt events is the most crucial factor that determines the total watershed solid yield. Therefore, different hydro-meteorological parameters such as total discharge, maximum discharge are typically preferred in TSS estimation models. Moreover, human activities along the stream network are more and more notably affecting TSS inputs. On the positive side, water conservation techniques are beneficial for fluvial system health. Whereas on the adverse side, dams and reservoirs construction, deforestation, intensive urbanization, mineral exploitation or construction works (Vercruysse et al. 2017, p. 41) result in soil and channel erosion which is recognized as a significant contributor to TSS load (Fox et al. 2016b, p. 604). Apart from that, land cover, urban runoff, WWTP and septic system effluents, and decaying plants and animals can affect the number of suspended solids into receiving waters (Murphy 2007c).

2.2.2. Nutrients

Nutrients, in appropriate amounts, are indispensable for vegetal photosynthetic processes and animal nourishment (Mueller and Helsel 1999b). Phosphorus and nitrogen usually are the most limiting and critical nutrients for algae and cyanobacteria production in surface waters and estuarial/coastal ecosystems respectively (Murphy 2007b). However, they can warrant concerns about a series of adverse consequences regarding the impaired ecological environment and threatened public health (Guan et al.

2016, p. 661). In particular, nitrates and phosphates are listed by the Water Framework Directive in the “Indicative list of the main pollutants” (2000/60/EC 2000).

The overabundance of nutrients is well-known as ‘eutrophication’ phenomenon. As defined by the Nitrate Directive (1991), eutrophication means ‘the enrichment of water by nutrient compounds, causing an accelerated growth of algae and higher forms of plant life to produce an undesirable disturbance to the balance of organisms present in the water and to the quality of the water concerned’ (91/676/EEC 1991). Reported by the US Office of Science and Technology, accelerated eutrophication in America was the major reason for the impairment of the nation’s rivers and streams, lakes and reservoirs, and estuaries (US EPA 1998). Later a great deal of literature has been published on the undesirable consequences, including not only decay of aquatic vegetation, oxygen deficiency, biodiversity loss (Lannergård et al. 2018, p. 104), but also noxious tastes and odors, clogged water-intake pipelines, constrained recreational values (Mueller and Helsel 1999a), as well as extra treatment costs for drinking water (Guan et al. 2016, p. 661). In order to avoid aforementioned negative aspects and to meet the clean water goals, justifying whether a waterbody is eutrophic in the first place and then understanding the main driving forces and influential factors that control the occurrence and deterioration of eutrophication are imperative.

To define a waterbody’s true biological productivity and choose sound management strategies (Richard, p. 4), trophic state criteria were developed by Forsberg and Ryding in 1980, based on four water quality parameters: total chlorophyll, total phosphorus, total nitrogen, and water clarity (Richard, p. 3). The Trophic State Index (TSI), on the scale of 0 to 100, was also designed by the Florida Administrative Code (FAC) to evaluate individual lakes, ponds, reservoirs and estuaries (Lake County Water Authority and USF Water Institute).

With respect to the main origins of nutrients, the European Environmental Agency has pointed out that in many catchments storm runoff passing by farming regions and effluent from sewage treatment plants were primarily responsible for nitrogen pollution, while industrial and domestic emitters were usually the most unignorable sources for phosphorus (European Environmental Agency 2018, p. 3). The primary factors that affect nutrient concentration in surface and sub-surface waters are land use, soil drainage capacity, geological status, and the distance to aquifer tables. To be specific, agricultural land and urban areas with intensive human activities accelerate eutrophication more efficiently than any other land uses; fine-grained silts and clays exert the largest retardment to nutrient movements downward to the underground; the groundwater from formations through which it penetrates fast, such as unconsolidated

sands and gravels, presents higher nutrient level (Mueller and Helsel 1999a). In the following sections, nutrient nitrogen and phosphorus will be outlined.

1) Nitrogen (N)

As a basic element, nitrogen exists either in organic forms acting as a necessary component within living organisms to assist the synthesis of proteins and peptides, or in inorganic forms including ammonia, nitrate (NO_3^-), nitrite (NO_2^-) and nitrogen gas (N_2) (Murphy 2007a).

NO_3^- is extremely soluble, stable and mobilizable in varying aquatic environment and can be easily consumed by phytoplankton and plants. It is capable of being quickly converted by Nitrobacter from NO_2^-, which is another soluble but more ephemeral nitrogen form. Attention has been drawn to the harmfulness, especially to infants who are more susceptible to blue baby disease, of NO_3^- and NO_2^- when they are excessively present in the potable water. Generally, NO_3^- concentration tends to be higher in groundwater situated under the areas of well-drained soils and intensive cultivation of crops than in streams (Mueller and Helsel 1999b).

Given the fact that ammonia is easily transformed to nitrate in oxygen-saturated conditions through nitrification and also likely to be converted to gaseous nitrogen when oxygen is absent in the water, it is believed that ammonia is the most unstable form of nitrogen in most natural waters. Depending upon the alkalinity and temperature of water bodies, two competitive forms, the ionic ammonium (NH_4^+), and dissolved unionized ammonia gas (NH_3) compete to be the leading one (Murphy 2007a). Relative to NH_4^+, NH_3 poses greater toxicity threat to wildlife by hampering hatching and growth processes and also to human beings, causing discomfort and even death.

Complying with pollution control policies, Germany was called on by the European Commission to take more operative measures to deal with the excessive release of nitrogen into groundwater and surface waters (The German Advisory Council on the Environment 2015). To this end, policymakers are supposed to comprehend the core emitters and determinants that control the amount and behavior of nitrogen throughout the fluvial channel, with keen attention to the potential processes that transfer large nitrogen loads (Alexander et al. 2009, p. 91).

First and foremost, farming use of nitrates in chemical fertilizers is responsible for more than half of the total nitrogen emission into surface waters in Europe (Iva 2010). Wastewater and septic system effluent, as point sources contain detergents and decomposition products of urea and protein from human wastes are recognized to be key sources of nitrogen. Animal waste, industrial discharge and combustion of fossil

fuels that release nitrogen oxide gases NO_x into the air and then trigger acid rain are all unneglectable contributors (Murphy 2007a). On the aspect of agricultural nitrogen inputs reduction, it is worth noting that agri-environmental measures, agricultural consultancy on water management issues and fertilizer legislation (The German Advisory Council on the Environment 2015) have been all-round established in Germany.
Nitrogen concentrations can suffer great fluctuation depending on the magnitude of hydrological events (Kulasova et al. 2012a, p. 1), biogeochemical parameters that control denitrification (Alexander et al. 2009, p. 92), the upstream land use (Mueller and Helsel 1999a), and the season.

2) Phosphorus (P)

Phosphorus is present in the aquatic environment either in particulate phases including phosphorus aggregates, phosphorus adsorbed to particles, and amorphous phosphorus, or in dissolved phases including organic phosphates and inorganic orthophosphates or polyphosphates (also acknowledged as metaphosphates or condensed phosphates) (Murphy 2007b). As the reactive and bioavailable form of phosphorus, orthophosphates ($H_2PO_4^-$, HPO_4^{2-}, or PO_4^{3-}) are the nutrients immediately taken up by bacteria and planktonic algae (Fox et al. 2016a, p. 607). They are able to be transformed from unstable polyphosphates, which are usually used in the production of detergents. Organic phosphates are formed via vital conversions from orthophosphates during biological processes or as a result of organic phosphatic pesticides degradation (Murphy 2007b). Compared to nitrate, phosphates tend to remain attached to soil particles due to their moderate solubility and mobility in the water and soils (Mueller and Helsel 1999a).

Phosphorus is concentrated in areas with frequent anthropogenic activities (Guan et al. 2016, p. 668) in that it is commonly contained in cleaning products and particularly fertilizers. After the application of phosphorus to arable land, typically in the form of commercial fertilizer or animal manure, it is subject to deposition, adsorption onto or detachment from particles (Hoffmann et al. 2009), or trapped by microorganisms or crop root systems, which is essential for agricultural production. However, when continuous fertilization is beyond plant uptake requirements, over-rich phosphorus in cultivated fields is harmful to the aquatic environment. Particularly, when the soil constitutes streambanks or is located in proximity to surface water systems (Fox et al. 2016a, p. 603), the potential of phosphorus desorption from soil particles and dissolution into waters will be enlarged once in contact with water (Beusen et al. 2005). Soil erosion of manured fields and grasslands can also convey a considerable amount of phosphates to watercourses with the aid of rainfall events or snow melting. Furthermore, via shallow groundwater transfer and tile-drainage, accumulated phosphorus can be remobilized and reach surface water bodies (Fox et al. 2016b, p. 604). Other contributors such as

animal waste, households and industrial wastewater effluent, phosphates mining or forest fires accelerate the concentration elevation of phosphorus in water bodies to different degrees (Murphy 2007b).

A wide range of studies have suggested that several influential factors inclusive of alkalinity, oxides and hydroxides of certain metals (calcium (Ca), iron (Fe), aluminum (Al)) (House et al. 1985), clay content and size, competitive adsorption of anions and retention time (Guan et al. 2016, p. 661) made a difference in the complex behaviour of phosphorus within hydrodynamic and biogeochemical systems, which also made the quantitative assessment of phosphorus a challenge.

Previous literature showed that total phosphorus was strongly linked to some other parameters like chl-a, turbidity, TSS, and Secchi disk transparency, which therefore were likely to be viewed as potential proxies for phosphorus (Gholizadeh et al. 2016). Namely, the real-time monitoring of phosphorus can be derived from its correlation with other easier reachable parameters rather than direct in-lab measurement. Even so, a time lag for aquatic biota to consume phosphorus, reported by Gholizadeh et al. (2016), made those correlations less unambiguous.

2.2.3. Turbidity

When an incident light enters a water body, it will partly subject to the absorption of suspended materials, partly transmit through the medium straightly, and partly scatter in various directions. Turbidity is the index that reflects the optical property of a medium in which light is spread and absorbed (Lawler 2016) rather than transmitted with no change in directions (Lawler 2014). It is reliant on the characteristics of the particles suspend inside e.g. water bodies, precisely SSC, grain size and shape, refractive index, and colority (Voichick et al. 2018, p. 1767). As a water cloudiness parameter, it is particularly beneficial for detecting abnormal physical changes in freshwater systems, indicating the environment degradation level resulting from suspended and colloidal substances in rivers and lakes, and useful for compiling reasonable water quality criteria in that it is well recognized that high turbidity can be related to elevated SSC in the water column (Rymszewicz et al. 2017, p. 100). Anomalous turbidity values can also trigger alarms so that drinking water intake structures can be in time shut down to avoid the breakdown of filtration systems. In the surrounding of natural water bodies, turbidity measurement is of importance to monitor and regulate construction works and dredging projects that cause turbidity (Voichick et al. 2018, p. 1768).

As defined in the standard EN ISO 7027, the turbidity of water can be determined by four procedures, in which transparency cylinder and sight disc procedures are based on visual comparisons and suitable for clean and slightly contaminated surface waters (Gudrun 2016). For water with low turbidity, nephelometry, as the third procedure,

directly assesses the degree of light scattering taking place in the medium (Lawler 2014) and the unit is given in Formazine Nephelometric Units (FNU or NTU). The apparatuses of a nephelometer are no different from a light spectrophotometer except that the detector is positioned at a specific angle from the incident light (Khouja 2000). The angle is contingent on at which direction most scattered light are received and it is usually, but not necessarily at right angles. Last but not least, turbidimetry is appropriate for water with low clarity (Gudrun 2016), e.g. municipal wastewater, industrial wastewater. In principle, it is involved with detecting turbidity by quantifying the attenuation extent of a beam of light with known initial intensity (Lawler 2014). The unit for turbidimeter detected values is given in Formazine Attenuation Units (FAU). Comparatively speaking, turbidimetry suffers greater sensitivity loss than nephelometry in a turbid suspension, because the intensity of transmitted light is much lower than the scattered light.

For both instruments, a single light source in the near-infrared wavelength range is applied and additional parameters frequently measured by the same instrument include temperature, electrical conductivity, and dissolved oxygen (Voichick et al. 2018, p. 1767).

2.2.4. Dissolved oxygen (DO)

For the purpose of quality classification of ecological status, the Water Framework Directive (WFD) has identified five ‘‘General chemical and physiochemical elements supporting the biological elements’’ for transitional and coastal waters (Best et al. 2007, p. 53), in which dissolved oxygen (DO) together with thermal conditions, salinity, acidification status and nutrient conditions are included (2000/60/EC 2000). Beyond that, oxygen deficiency has been recognized as an indirect indicator of nutrient enrichment.

DO is commonly expressed either as a mass/volume metric (mg/L) or as a saturation percentage (%) (Best et al. 2007, p. 56). Nitrification and respiration consume oxygen and photosynthesis producing oxygen are two key factors that govern DO concentration in the water, whereas the major physical indexes of water bodies that influence DO are temperature and salinity: DO solubility declines with growing temperature and salinity (Best et al. 2007, p. 54).

The measurement of DO in waters has changed over the years from determined iodometric titration of the water sample, which is widely known as the Winkler method, to electrochemical and optical methods that enabled real-time and long-term monitoring of its spatial heterogeneity and temporal dynamics (Rajwa et al. 2014, p. 343).

2.2.5. Water quality criteria and directives

Concerns about nutrient pollution resulted in political actions, translated into legislative directives such as the Clean Water Act (1972) in the US (Ferreira et al. 2011), in which nutrients in sewage effluent were listed among the primary pollution-control targets (Mueller and Helsel 1999a).

Requested by Safe Drinking Water Act in 1974, the US EPA has set an enforceable maximum contaminant level goals (MCLG) for nitrite and nitrate in drinking water at 1 mg/L and 10 mg/L respectively (US EPA), to protect human health. The EPA also recommended that “total phosphate should not exceed 0.05 mg/L (as phosphorus) in a stream at a point where it enters a lake or reservoir, and should not exceed 0.1 mg/L in streams that do not discharge directly into lakes or reservoirs” (Murphy 2007b).
In 1991, the EU introduced the Nitrates Directive, which was one of the earliest pieces of EU legislation aiming “to safeguard other legitimate uses of water and to reduce water pollution caused or induced by nitrate from agricultural sources and prevent further such pollution” (European Environmental Agency 2018, p. 3).
The Urban Waste Water Treatment Directive (91/71/EEC) demanded a reduction in nutrient discharges from point sources and required the identification of vulnerable zones (European Environmental Agency 2018, pp. 2–3).
In 1994, EPA commissioned a research on State Water Quality Criteria and Standards for Nutrients (US EPA 1998). In the sequence, the 1998 Clean Water Action Plan initiated the establishment of nutrient criteria to protect and restore American waters in a more manageable way (Evans-White et al. 2013, p. 1002).
In 2000, the WFD requires the achievement of good ecological status and good ecological potential of rivers across the EU by 2015 (European Environmental Agency 2018, p. 3), and included nutrients as one of the most important parameters to determine ecological status of water bodies (2000/60/EC 2000).
By contrast, the Marine Strategy Framework Directive (MSFD, 2008) paid special attention to the eutrophication level assessment for all the European marine waters (Ferreira et al. 2011).
Later on, phosphorus standards recommended by the UK Technical Advisory Group have been used to indicate the probable degree to which phosphorus concentration needs reduction (Pollard 2013).

From the perspective of TSS, since the inclusion of solids in the EPA Quality Criteria for Water in 1986 (US EPA 2003, p. 15), a wide range of standards have been compiled, regarding turbidity as a surrogate measure or using narrative criteria (Berry et al. 2003, p. 17)

3. Methodology

In this chapter, the concepts and steps of three load estimation approaches and an emission model are specified. Hilden approach was developed in 2003 as a simple scaling reference. As for LVS-based approach, with a flow-proportional collection of samples into a large in-field sampler, it generated 18 regression models and utilized two

sub-methods to conduct budgeting. Last but not least, the turbidity-based approach had the chance to accomplish mass balance in a simple way, that is, continuous detection of turbidity as an indicator of SSC. The timescales associated with these methods are illustrated in Figure 3.1.

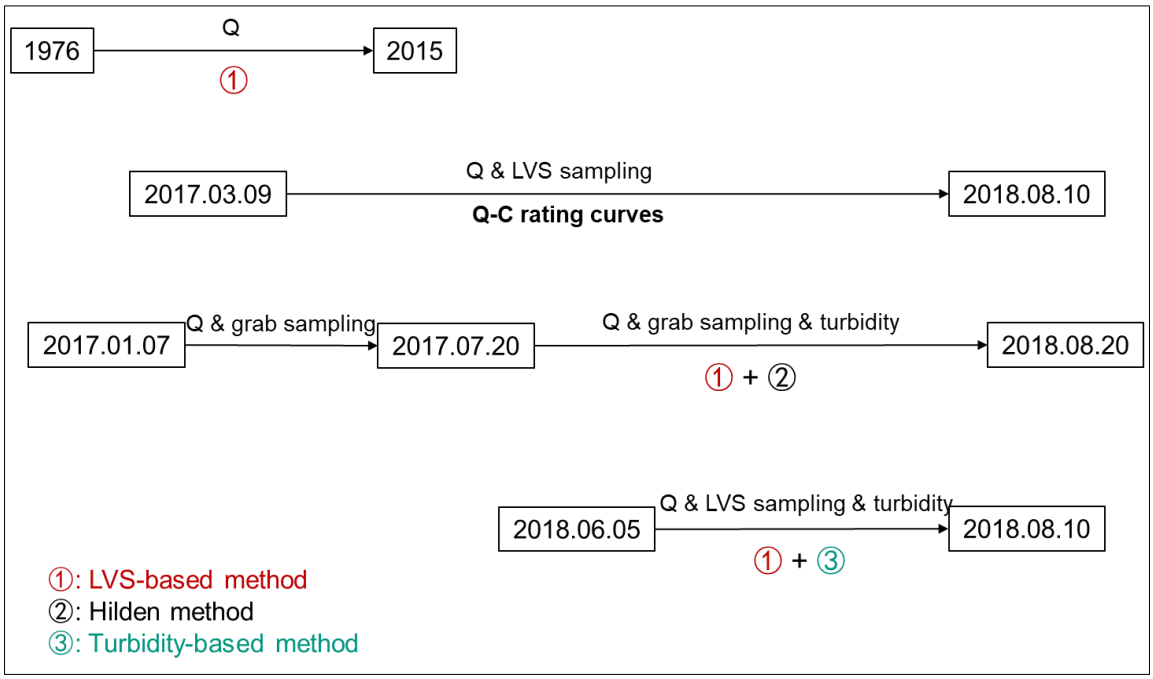

Figure 3.1 Timescales and associated methods. Discharge Q was constantly measured at a frequency of 15 minutes.

3.1. Hilden approach

In our cases in the Kraichbach catchment, grab samples, in all 23, were retrieved on an irregular regime, with time interval ranging from days to months. Analyzed water quality parameters from these grab samples included TSS, NO_3-N, NO_2-N and NH_4-N, TP and PO_4-P. Their mean concentrations and simultaneously recorded water discharges (Qi) were applied into Equation 3 to calculate the standard annual load F. Next step was to determine the correction factor, which was the ratio of the overall mean discharge $\bar{Q}$ in the year of observation and the mean sampling discharge Q_M as described in Equation 4 and Equation 5. Lastly, corrected annual load F_Q was calculated by Equation 6.

In this thesis, Hilden approach was further adjusted. Conventionally, the correction factor is relevant to $\bar{Q}$ as described above. However, to emphasize the influence of peak events, $\bar{Q}$ was replaced by Qp, the mean value of the highest p% discharges in the year of interest. The determination of p values depended on the deviation of Hilden estimates from the “true loads” (LVS-based results). For instance, if the “true load” was m-times larger than Hilden estimate, then the ratio of Qp and $\bar{Q}$ should be equal or close to m.

3.2. LVS-based approach

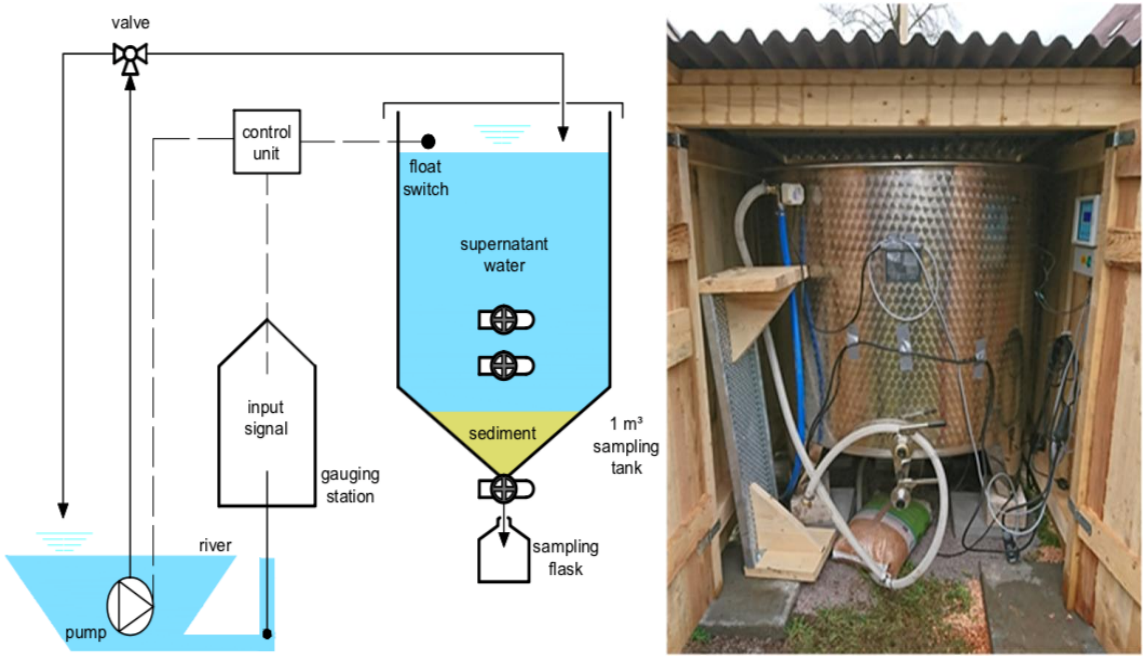

Figure 3.2 Sketch (left) and photo (right) of the Large Volume Sampler (IWG-SWW 2018)

The Large Volume Sampler (LVS) is located at a Kraichbach gauging station in Ubstadt Weiher. This 1000-Liter-tank has performed 26 periods between Mar. 2017 and Aug. 2018 (measurements still ongoing). Each sampling period lasted on average for 10 days long (ranging from 6 to 18 days), during which discharge-proportional mixed samples were collected. To be specific, more river water will be retrieved in high flow conditions than in low flows. Consequently, the mean concentration measured in the tank was regarded as a close approximation of the mean concentration in the river during the sampling period, which allowed for much more robust estimates of sediment fluxes, in comparison to grab samples (IWG-SWW 2018).

In a standard sampling event (without the consideration of half-full and over-full incidents), the intake pump worked averagely 82 times (in the range of 68 to 103), withdrawing 12.2 L river water per time. Meanwhile, on average roughly one million cubic meter river water passed through the monitoring station. Based on its working schedule and intrinsic principle, Time-split and Volume-split methods were separately developed to cope with the mass balance.

The main idea of this method was to construct rating curves that described the correlation between the highest discharge values and the measured mean concentrations (fluxes) of selected parameters within all the LVS sampling periods. Thus, further concentrations (fluxes) and masses can be predicted with a considerably reduced amount of efforts by simply discharge detection. For Kraichbach, mean total suspended solid flux (TSS, g/s), total nitrogen concentration (TN, mg/L), particulate nitrogen flux

(N_part, mg/s), dissolved nitrogen concentration (N_dis, mg/L), total phosphorus flux (TP, mg/s) and particulate phosphorus flux (P_part, mg/s) were the priority focuses.

After the build of models, determining the best logically and statistically performed one for each study parameter (Sadeghi et al. 2008, p. 199) is important. The upper end of water discharge was recorded as 7.8 m^3/s during event Nr. 21, and these models were not calibrated for higher flows. Therefore, any flow rates higher than 7.8 m^3/s will be mandatorily assigned to be 7.8 when models were put into use. Therefore, generated rating curves will be conditional. Depending on accessible datasets, time frames for each parameter slightly varied.

In order to select better regression curves, several estimating model criteria were referred. Regression formulas, the coefficient of determination (R^2) and root mean square error (RMSE) are shown near the curves, which were all visualized by R programming language.

The coefficient of determination, denoted by R^2, is given by

$$R^2 = 1 - \frac{SSR}{SST}$$

(Equation 7) (Devore 2012, p.485)

Where SSR is residual sum of squares; SST is the total sum of squares.

R^2 is interpreted as the degree of observation variation that can be attributed to a linear regression model. It is in the range of 0 and 1 and higher value of R^2 infers a more successful model (Devore 2012, p. 485).

RMSE shares the unit of measurement with observed objects. As a more omnibus measure of goodness of fit, it is applicable to not only linear models but also exponential, hyperbolic and other models.

$$RMSE = \sqrt{\frac{\sum (X_{pi} - X_{ti})^2}{N}}$$

(Equation 8)

Where N is the sample size; $X_{pi} - X_{ti}$ is the difference between predicted and true values.

Nonetheless, when it comes to the comparison among datasets or models with various orders of magnitude, it is not sufficient to only count on RMSE. As a supplement, dimensionless RMSE* comes into use. Typically, RMSE* is the normalized RMSE by the mean value or the range (the difference between maximum and minimum values). In our case, RMSE* is defined as:

$$RMSE^* = \frac{RMSE}{C_{max} - C_{min}}$$

(Equation 9)

Developed models are specialized for the Kraichbach catchment in current hydrological and geological conditions, and it is prerequisite to re-calibrate prior to any employment once significant changes have occurred.
During the application of rating curves, two sub-methods were adopted to generate the maximum water discharge series and they are specified beneath.

3.2.1. Time-split method (T-split)

On the average, LVS was emptied and started to rerun every 10 days. The main idea behind the Time-split method (T-split) is to figure out the mean concentration (flux) via the largest discharge value in every 10 days with the assistance of established rating curves (Figure 3.3). Accordingly, the transported mass can be deduced. T-split was derived from the LVS operation schedule, as an empirical reference, it is uncomplicated to compute but not so plausible. The reason is that it was based on an inconstant duration time. As a matter of fact, the operation interval was not exactly 10 days. Instead, it varied from 6 to 18 days, depending on how long did it take for a constant volume of river water to pass by. Therefore, another more reliable method was parallelly developed.

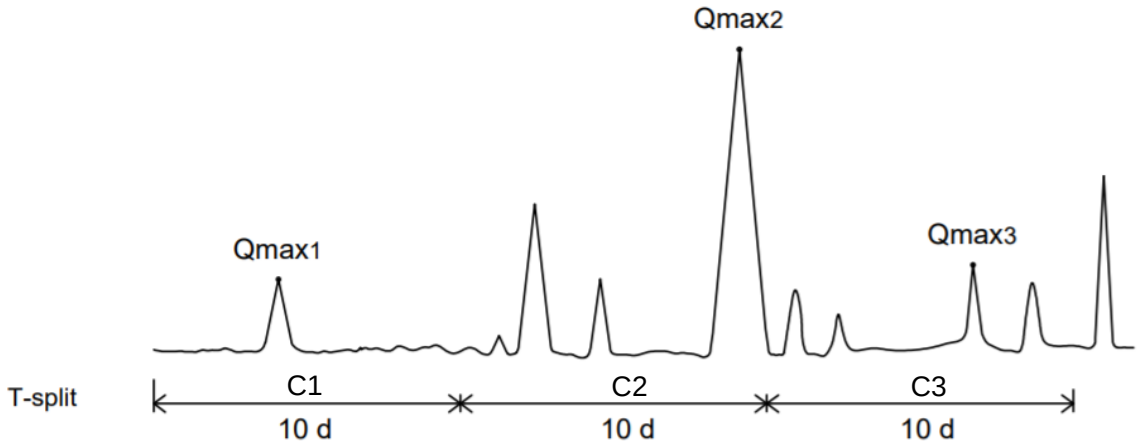

Figure 3.3 Sketch of Time-split method principle. The sampling duration is constantly 10 days. C_N is the mean concentration (flux).

3.2.2. Volume-split method (V-split)

Rather than the division of obtainable discharge datasets by a definite time interval, the start point of the Volume-split method (V-split) is to divide them into several independent parts by a specific volume value, 1096151 m^3 in this thesis to be exact, and then seek for the highest flow in each individual part (Figure 3.4). Explicitly, the largest discharges will be immediately determined every time when the river water has passed the gauging station for 1096151 m^3. This specific value was calculated from the mean water volume passing by during all the standard events when LVS was neither half- nor over-filled.

Technically, V-split was the most trustworthy method due to the fact that it was developed based on the identical inherent principle to that of LVS and took the importance of actual flow conditions into consideration.

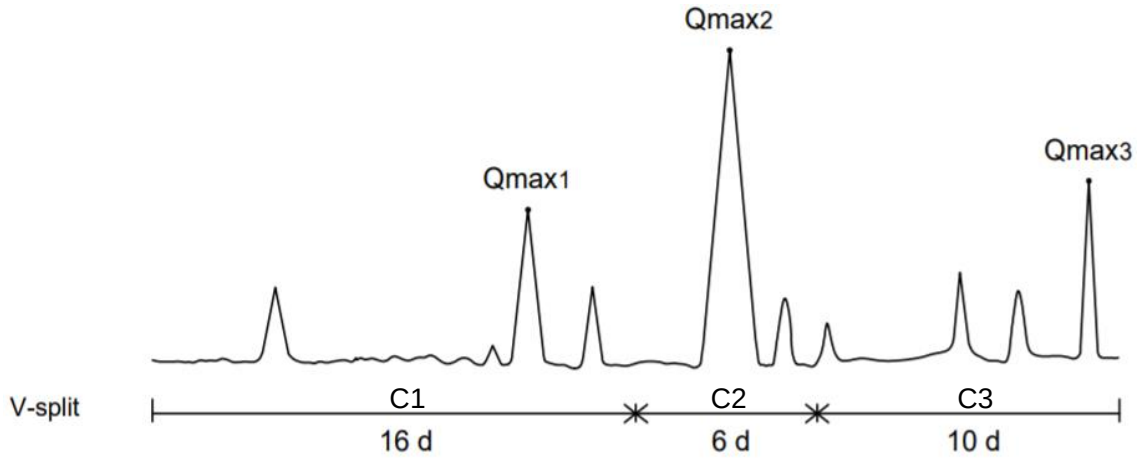

Figure 3.4 Sketch of Volume-split method principle. Dependent on flow conditions, the length of sampling duration is inconstant, that is, longer in dry days and shorter in wet days. C_N is the mean concentration (flux).

3.3. Turbidity-based approach

In this thesis, in-situ detected turbidity values (recorded as sensor signals, in arbitrary unit (a.u.)) and matched sediment concentrations were combined to build a regression model. On the basis, continuous SSCs became accessible through continuously detected turbidities. Simultaneously monitored discharges were then required to produce the resultant sediment budgets.

3.4. MoRE model

MoRE model for the Kraichbach catchment has been established during years 2009-2014. It focused attention on following pathways: atmospheric deposition (AD), decentralized households systems (DCS), erosion based on the sediment input of 938.5 t/a (Er), groundwater (GW), industrial discharges from factories (ID), interflow (IF), urban systems consisting of combined sewer overflows and separate sewer system spillways (US), surface runoff from arable land and pastures (SR), tile drainage of agricultural land (TD), WWTP and so forth (Figure 3.5). The arable land erosion was provided by Company GALF (Dresden) based on the soil loss map given by Landesamt für Geologie, Rohstoffe und Bergbau (GALF 2018). Three water quality parameters were included: TP, PO_4-P and TN.

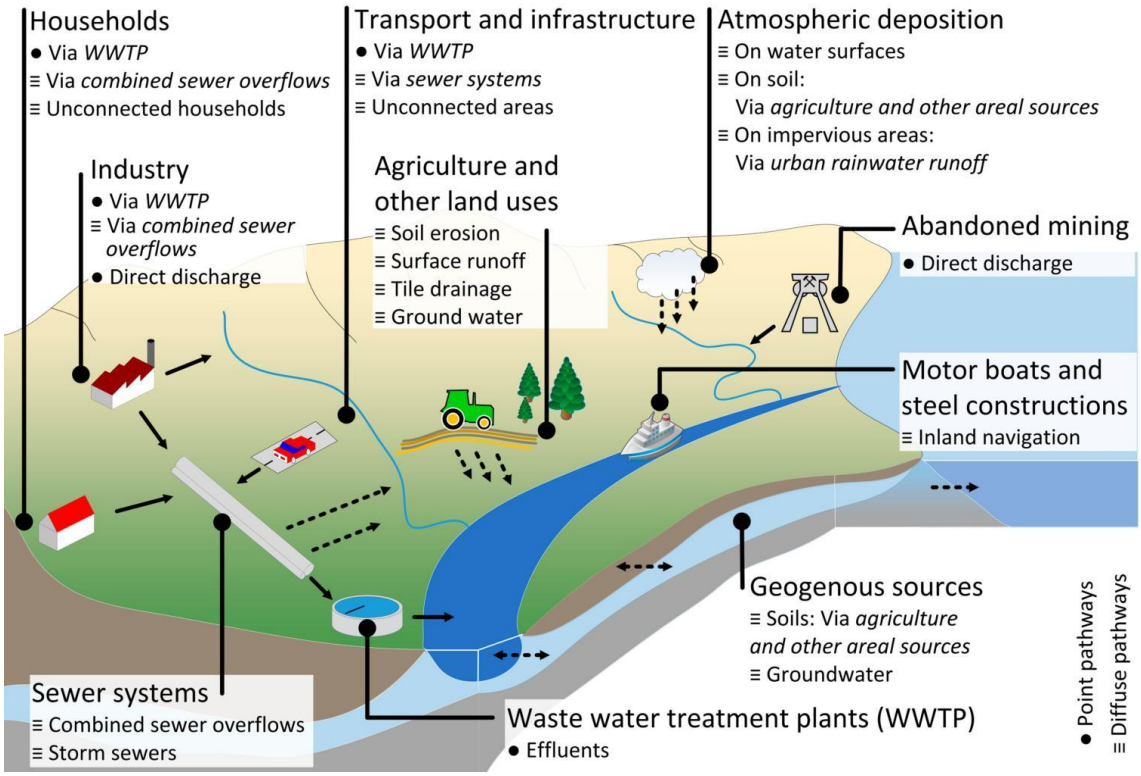

Figure 3.5 Pathways included in Modeling of Regionalized Emissions (MoRE) model (Fuchs et al. 2017)

4. Characterization of available datasets

The processing of the data, statistical computations and plotted graphs were mostly achieved by the R language and environment.

4.1.1. Hydrological values

When it comes to the design of hydraulic structures or scientific assessment of river utilization, the hydrological values concerning water discharge become decisive (Ihringer and Liebert 2015). To conduct the regional hydrological research, in cooperation with the Institut für Wasser und Gewässerentwicklung (IWG) Bereich Hydrologie of the Karlsruhe Institute of Technology (KIT), the Landesanstalt für Umwelt, Messungen und Naturschutz Baden-Württemberg (LUBW) provides hydrological values inclusive of HQ_T (T-jährlicher Hochwasserabfluss), MNQ (Mittlerer Niedrigwasserabfluss), MQ (Mittlere Abfluss) and MHQ (Mittlerer Hochwasserabfluss) (Ihringer and Liebert 2015). Along with water levels, they are listed on the online portal “Hochwasservorhersagezentrale Baden-Württemberg”, where the latest discharge is updated every 15 minutes.

To be precise, MNQ, MQ and MHQ are statistical values. MNQ and MHQ stand for the mean value of the lowest and highest discharge respectively for a defined observation

period, while MQ reveals the mean value of all discharges in the interval (Kentroti 2017, p.24). They were updated by LUBW-MNQ-Regionalisierung on 14. Jan 2015 (LUBW 2018). Based on historic data denoting the average recurrence interval of a flood flow, HQ_T theoretically reveals the topmost flow that happens only once in T years. They are required to be decided cautiously for accuracy and completeness since they are linked to risk prediction. HQ_2, HQ_{10}, HQ_{20}, HQ_{50}, HQ_{100} for Ubstadt Kraichbach were updated by LUBW-MNQ-Regionalisierung on 03. Dec 2013 (LUBW 2018).

Hourly averaged discharge values at different temporal scales were classified in terms of these hydrological values. However, in the view of the fact that the magnitude and true values of MHQ and HQ_2 did not differ for most gauging stations (Kentroti 2017, p.24), and so as to achieve less complicated classification, it was more appropriate and reasonable to choose only one of them (Kentroti 2017, p.25). It made more sense that HQ_2 was selected rather than MHQ since the maximum discharge occurred and employed for LVS model development was 7.8 m^3/s, which is closer to HQ_2.
Additional, discharge values were defined by the percentiles from 0 to Q100, which were calculated based on the discharge datasets in 1976-2015. This was partly for the aim of the river's hydrological status evaluation and partly aiming at the analysis of the contribution of low-flow and peak events.

Table 4.1 Hydrological values (m^3/s) of Kraichbach (source of data: LUBW 2018)

MNQ	MQ	MHQ	HQ_2	HQ_{10}	HQ_{20}	HQ_{50}	HQ_{100}
0.62	1.10	8.63	7.79	14.20	16.70	20.10	22.70

Table 4.2 Discharge percentiles (m^3/s) of Kraichbach in 1976-2015 (source of data: LUBW 2018)

Q10	Q20	Q30	Q40	Q50	Q60	Q70	Q80	Q90	Q100
0.603	0.713	0.789	0.878	0.976	1.075	1.207	1.341	1.661	26

4.1.2. Discharge data

Discharge at Ubstadt Gauge is measured and updated by LUBW at a frequency of 15 minutes, but the mean hourly discharge values are used for analysis in this thesis.
For different purposes, overall discharge data were divided into four parts and applied to rating curve models individually. During the time window from 1976 to 2008, they were used to generate the sediment concentrations and budgets. Note that is was assumed that catchment properties and stream morphology remained the same as it has been since 2009. Likewise, relevant results may be considered as the prediction for years with similar flow conditions to selected years. In the period of time from 2009 to 2015, erosion protection measures have already been accomplished in the catchment of interest. After

that, the Kraichbach catchment stayed in a relatively stable status. In parallel, a sediment and nutrient input model has been built to simulate the emission situation and served as a reference. From July 2017 to July 2018, when the LVS intermittently functioned and grab samples were in the meantime analyzed, LVS regression models and Hilden approach were both conducted for comparison purpose, in terms of annual masses of SS, P, and N species. Lastly, two months in the summer of 2018 were selected to testify the feasibility of a turbidity-based approach.

Minimal, maximal, mean flows and overall sample size are descriptive statistics to quantitively characterize flow measurements. They assist, to some extent, a better selection of models for the observation period according to the model's application range. The annual sample size was always 8759 or 8783 depending on it was a common or leap year.

Statistical measures such as median, interquartile ranges (IQR), standard deviation (STD), are used to assess the spread of discharges, describing a great number of datasets in a succinct way. IQR is defined to be the subtraction of Q_{75} and Q_{25} percentiles, therefore it measures the central 50 shares of the entire data and remains resistant to the impact of the 25 percent on either extreme end (Helsel Hirsch 2002, p.8). STD is the (positive) square root of the variance (Devore 2012, p. 36). Smaller-magnitude STD is an indication of less variability of samples.

Table 4.3 Statistical values of discharge (m^3/s) in different timescales (source of data: LUBW 2018)

Timescale	N	Qmin	Qmax	Qmean	Qmedian	IQR	STD
1976-2015	350600	0.15	26	1.1	0.98	0.53	0.71
2017/2018	8757	0.29	7.79	1.21	1.12	0.67	0.64
2018.06-.08	1465	0.6	3.62	1.01	0.93	0.25	1.00

1) Years 1976- 2015

Figure 4.1 illustrates the flow rate distribution during the 40 years from 1976 to 2015, including dry years like 1991 and 1977, and wet years like 1988, 2002, when above-HQ_{100}-floods occurred.

During this period of time, discharge values have been recorded 350600 times, in which fluxes higher than HQ_{10} happened rarely, 43 times in all. Slightly more than half of the flows fell into [MNQ, MQ) class, followed by [MQ, HQ_2) class. All in all, most of the event fluxes were below HQ_2.

Due to considerable outliers existed in 2002, they brought a comparable water volume as in 1983 and 1988, even if this year presented narrower distribution in [MQ, HQ_2) class.

In 1991, 52% of flows were lower than MNQ, inducing the least water volume, which made it the acridest year during the 40 years.

Judging from slightly higher mean discharge than the median, the overall distribution was somewhat skewed to the right.

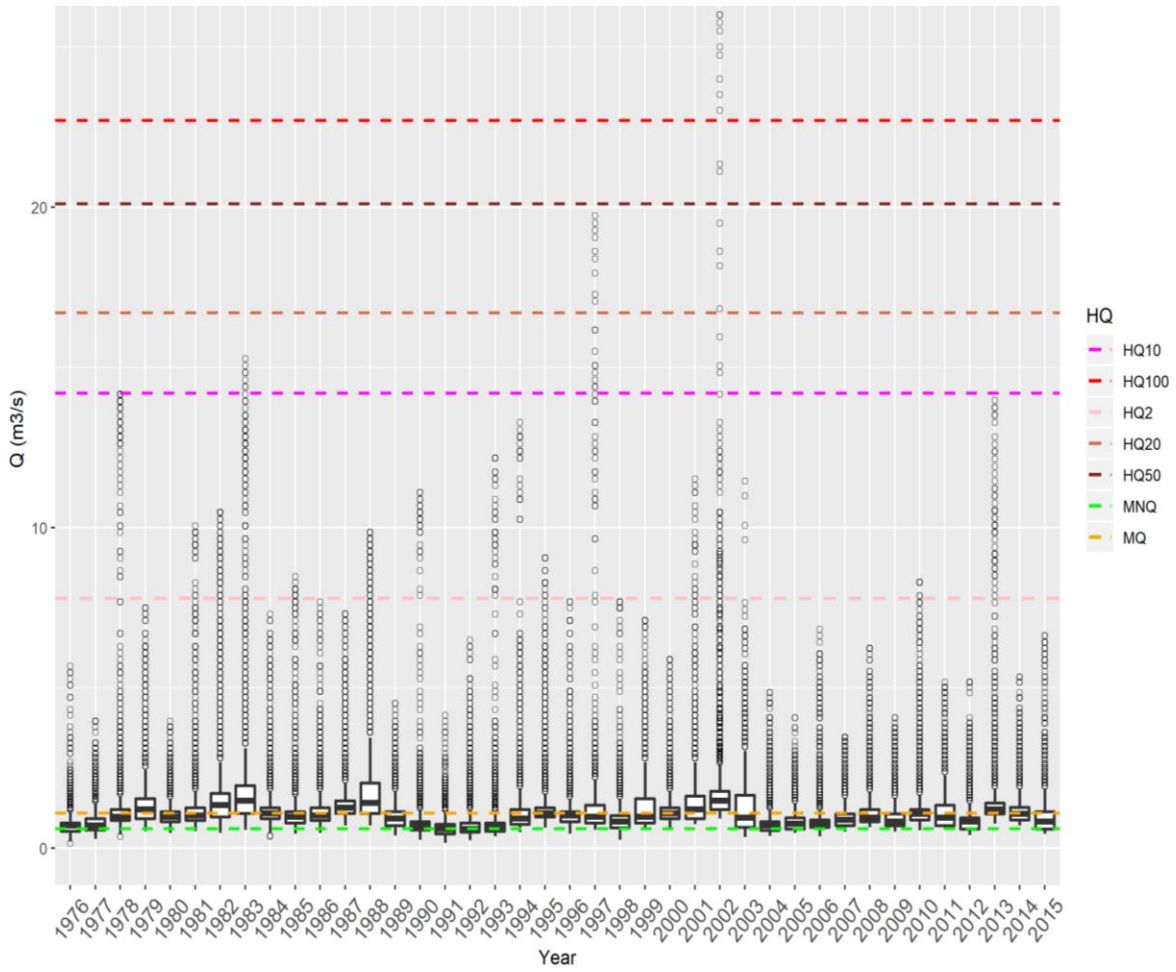

Figure 4.1 Annual flow rate distribution of Kraichbach in 1976-2015. The horizontal lines represent the characteristic hydrological values including MNQ (mean low flow), MQ (mean flow) and HQ_T (highest flow in T years) (source of data: LUBW 2018).

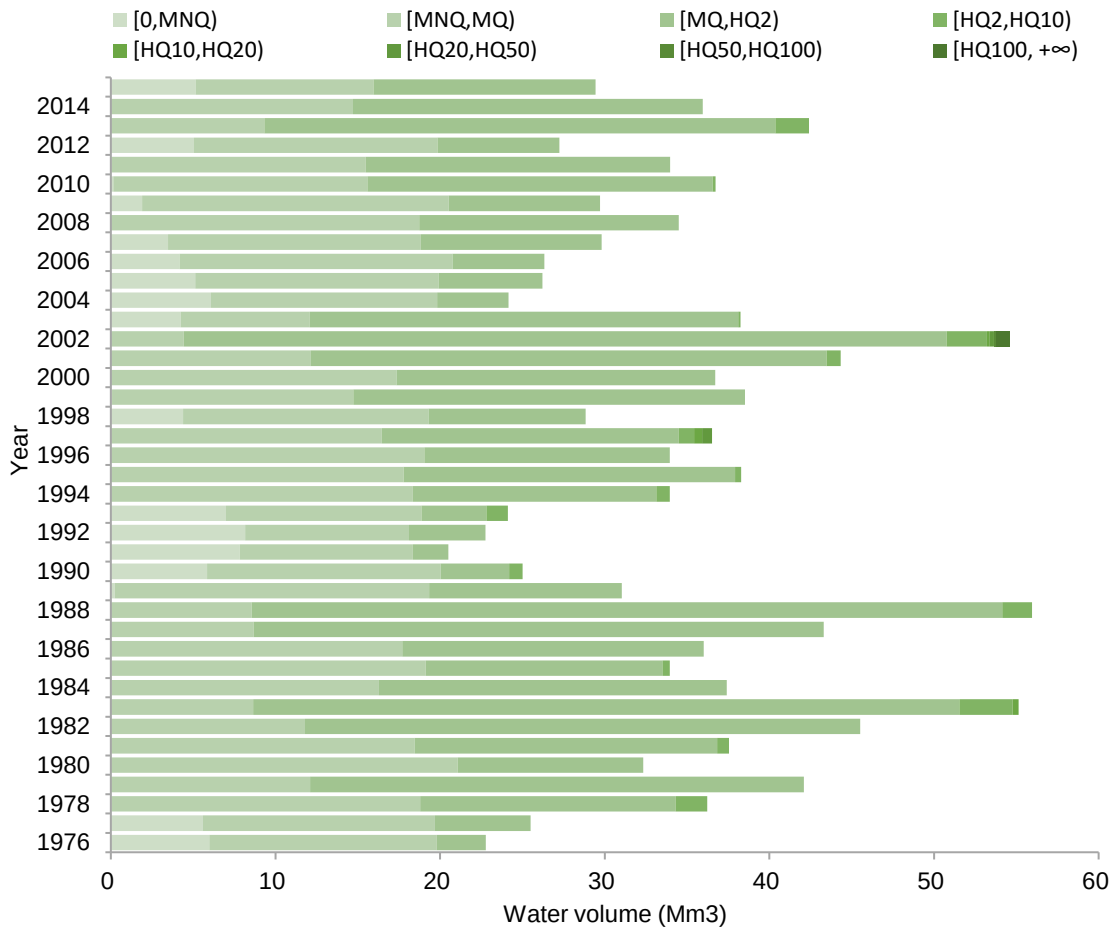

Figure 4.2 Annual water volume (m^3) and constitutions in Kraichbach during 1976-2015 (source of data: LUBW 2018)

2) Year 2017/ 2018

The year 2017/2018 was selected to compare the budgets from LVS-based and Hilden methods. The period of time started on 20th of July 2017 and lasted for a whole year until 20th of July 2018, counting discharge 8757 times. The greatest flow, slightly lower than HQ_2, happened only once. The discharge was skewed a little bit to the right. In this time frame, grab samples were manually collected as shown in Figure 4.3 by the red crosses. However, it is obvious that the vast majority of grab samples were gathered at low flow conditions, which undeniably brings bias into further calculations.

3) The summer of 2018

In 2018, two months from 5th June to 10th August focused on a feasibility study of turbidity as an optical index to indicate SSC, during which turbidity loggers were installed. Flow conditions varied to a certain degree but remained always below HQ_2, with the highest discharge of only 3.6 m^3/s.

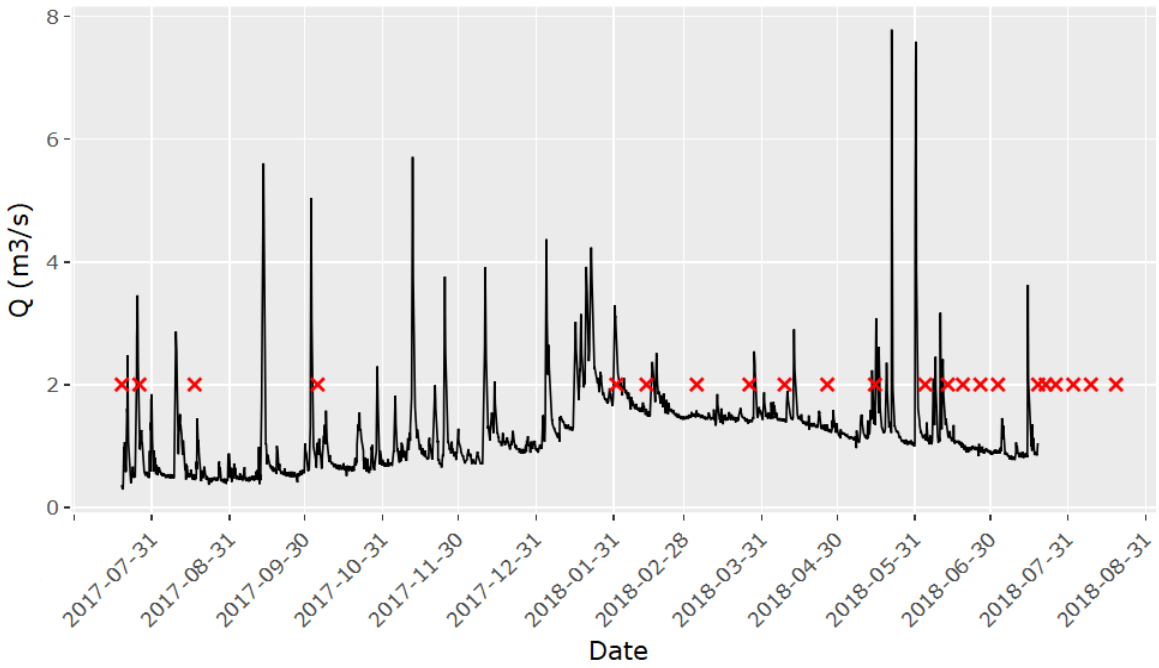

Figure 4.3 Hydrograph of Kraichbach for the year 2017/2018, starting on 2017.07.20 and ending on 2018.07.20. The timepoints of discrete grab sampling are denoted by red crosses (source of data: LUBW 2018).

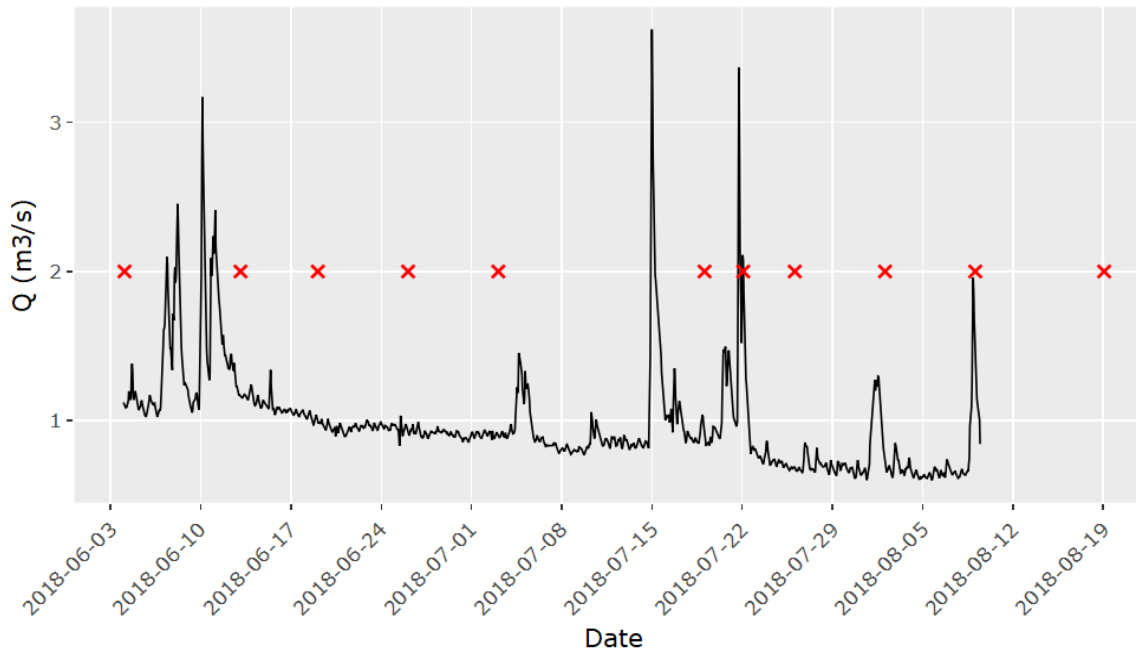

Figure 4.4 Hydrograph of Kraichbach for the period of 2018.06.05-2018.08.10. Red crosses indicate the date when in-situ turbidities were also measured during sampling (source of data: LUBW 2018).

Table 4.4 Grab sample water quality. "-" means data were not available; Turbidity values were expressed as sensor signals in a.u. (arbitrary units) (source of data: IWG-SWW 2018).

Date	Time	SSC (mg/L)	TP (mg/L)	PO_4-P (mg/L)	NO_3-N (mg/L)	NO_2-N (mg/L)	NH_4-N (mg/L)	Turbidity (a.u.)
2017-01-17	10:53	12.2	-	-	-	-	-	-
2017-07-20	16:40	17.2	0.22	0.16	-	-	-	-
2017-07-27	15:17	39.0	0.30	0.18	-	-	-	-
2017-08-18	10:45	26.0	0.18	0.12	6.8	0.04	-	-
2017-10-06	14:20	43.2	0.31	-	5.4	0.04	-	-
2018-02-02	14:28	31.3	-	-	5.8	-	0.24	-
2018-02-14	11:21	13.5	-	-	6.7	0.12	0.12	-
2018-03-06	12:55	11.2	-	-	6.6	0.13	0.13	-
2018-03-27	14:13	8.1	0.12	0.09	7.1	0.18	0.08	-
2018-04-10	11:30	14.7	0.09	0.09	6.7	0.08	0.05	-
2018-04-27	13:30	13.8	-	-	6.4	0.13	0.06	-
2018-05-16	12:40	74.5	-	-	5.1	0.22	1.13	-
2018-06-05	12:40	43.4	0.22	0.13	7.2	0.24	0.11	214.0
2018-06-14	16:00	100.2	0.31	-	-	-	-	152.8
2018-06-20	14:30	29.8	0.24	0.16	6.8	0.33	0.12	143.1
2018-06-27	13:20	19.3	0.20	0.15	7.3	0.30	0.21	97.6
2018-07-04	16:20	17.9	0.23	0.16	7.4	0.40	0.19	116.2
2018-07-20	13:12	32.4	0.23	0.18	-	-	-	146.7
2018-07-23	13:00	107.4	0.33	0.14	-	-	-	516.6
2018-07-27	17:00	29.9	-	-	-	-	-	119.7
2018-08-03	9:55	26.7	0.27	0.19	-	-	-	161.5
2018-08-10	11:40	42.2	0.27	0.16	-	-	-	48.2
2018-08-20	14:00	21.4	0.20	0.15	-	-	-	270.3

4.1.3. Grab sample measurements

Samples have been taken since January 2017 and stopped for six months in a row. In later 2017 they were sparsely collected and then stopped for another four months again. In contrast, they were more regularly analyzed in 2018 at an average frequency of three times a month. The SSC, nitrate nitrogen (NO_3-N), nitrite nitrogen (NO_2-N) and ammonia nitrogen (NH_4-N), total phosphorus (TP) and phosphates (PO_4-P) were measured in mg/L in laboratory immediately after collection in case of degradation. COD (chemical oxygen demand) and DOC (dissolved organic carbon) were measured but excluded from Table 4.4**,** since they did not display any apparent links to other parameters or discharges.

As described in Chapter 3.1.1, grab sample results are of significance for Hilden approach, hence the fluvial loads for listed parameters can be determined. PO_4-P, the dissolved and reactive phosphorus form has been determined by Hilden approach, but particulate phosphorus, as the difference between TP and PO_4-P, was the one that was compared with the outcome from other LVS-based methods.

4.1.4. LVS measurements

Formerly mentioned 26 LVS events are listed in Table 4.5 including the beginning and end date and time, duration in days, and corresponding hourly maximum discharge values (Qmax_h, m^3/s). During events Nr. 10, Nr. 23 and Nr. 24, the intake pump worked only around 46 times so the LVS was only half-filled. On the contrary, over full situation happened in event Nr. 16 with 149 times of pumping and in the interim more than two million cubic meters of river water has passed by. As possible sources of error, these four events were excluded from the determination of the specific water volume applied in the V-split. Except for a flood event Nr. 21 occurred in May 2018, the river flow condition remained in a relatively low state.

Both concentrations in mg/L and flux in mg/s of water quality parameters were measured. Depending on suitability for model development, optimum units of measurement were then differentiated, that is, N_dis and TN were investigated by concentrations while others by fluxes.

The correlation among the parameters of interest was studied as illustrated in Figure 4.6 and the degree of correlation was demonstrated by correlation coefficients in grids. The correlation coefficient of parameter X and parameter Y, denoted by Corr (X,Y), ρ (x,y) or just ρ, is defined by:

$$\rho\,(x,y) = \frac{\mathrm{Cov}\,(X,Y)}{\mathrm{sd}(X) * \mathrm{sd}(Y)}$$

(Equation 10)

Where Cov (X,Y) is the covariance between X and Y.

ρ (x,y) is a measure of the linearity between X and Y. When ρ = 0, X and Y are defined to be linearly uncorrelated, but it does not imply that X and Y are independent since there might still be a strong nonlinear relation**.** A ρ close to 1 in absolute value indicates only that the relationship is completely linear (Devore 2012, p. 210).

Beyond all question, fluxes of particulate nutrients and sediment tended to exhibit significantly strong and positive internal relations. TN and N_dis fluxes were highly linked to each other, too.

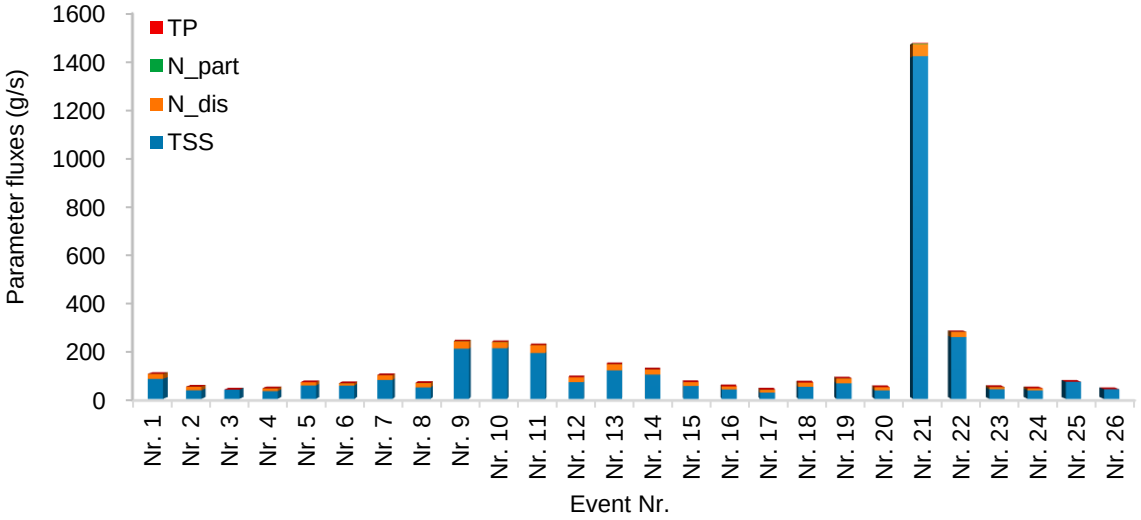

Figure 4.5 LVS measurement results of 26 events for TSS, N and P (source of data: IWG-SWW 2018).

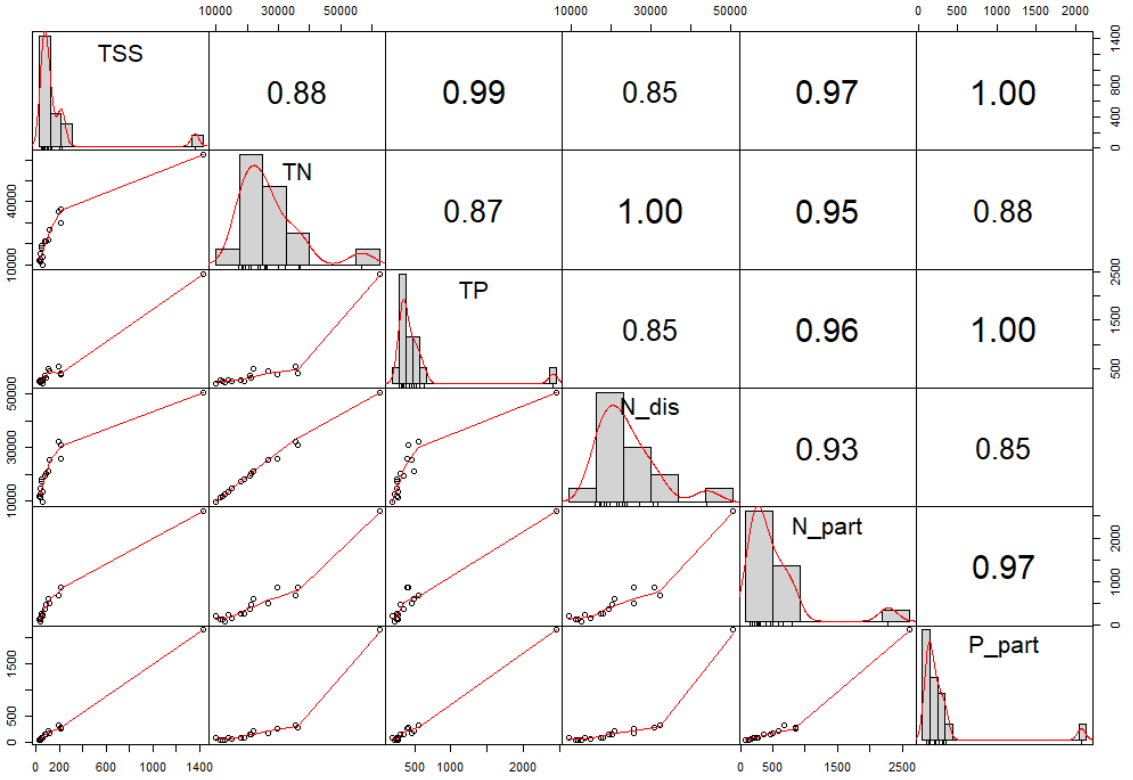

Figure 4.6 Correlation among the fluxes of water quality parameters in LVS (TSS: g/s, others: mg/s). The numbers in grids are correlation coefficients between parameters calculated by the R project.

Table 4.5 Large Volume Sampler operation events. V (m^3) is the volume of river water that has passed by during events (source of data: IWG-SWW 2018).

Event Nr.	Start	End	T (day)	Qmax (m^3/s)	V (m^3)
Nr. 1	2017-03-09 16:36	2017-03-16 12:32	7	3.3	917902
Nr. 2	2017-03-21 15:43	2017-03-29 09:38	8	2.1	921869
Nr. 3	2017-04-05 12:07	2017-04-14 12:58	9	1.2	905444
Nr. 4	2017-04-27 14:38	2017-05-06 20:46	9	1.6	947526
Nr. 5	2017-05-16 14:46	2017-05-27 03:51	11	1.8	905551
Nr. 6	2017-06-08 15:24	2017-06-23 17:29	15	1.3	949706
Nr. 7	2017-07-11 14:56	2017-07-27 08:51	16	3.5	1048202
Nr. 8	2017-08-08 11:24	2017-08-21 14:26	13	2.9	934889
Nr. 9	2017-09-05 14:07	2017-09-20 06:12	15	5.6	1107203
Nr. 10	2017-09-29 10:18	2017-10-07 00:00	8	5.0	689940
Nr. 11	2017-11-03 15:31	2017-11-13 07:31	10	5.7	1022550
Nr. 12	2018-01-10 11:59	2018-01-18 10:05	8	3.0	1089813
Nr. 13	2018-01-22 11:27	2018-01-29 11:07	7	4.2	1380171
Nr. 14	2018-01-31 17:32	2018-02-06 07:55	6	3.3	1047180
Nr. 15	2018-02-12 14:32	2018-02-19 12:29	7	2.5	1073516
Nr. 16	2018-02-22 15:59	2018-03-10 04:25	16	1.7	2009631
Nr. 17	2018-03-14 14:18	2018-03-24 03:58	10	1.6	1214969
Nr. 18	2018-03-27 13:55	2018-04-05 18:20	9	2.5	1257326
Nr. 19	2018-04-10 10:25	2018-04-19 15:13	9	2.9	1243807
Nr. 20	2018-04-27 10:56	2018-05-09 10:44	12	1.6	1245756
Nr. 21	2018-05-16 12:08	2018-05-24 21:45	8	7.8	1253637
Nr. 22	2018-06-05 10:44	2018-06-15 19:20	10	3.2	1245648
Nr. 23	2018-06-20 13:11	2018-06-27 11:16	7	1.0	568110
Nr. 24	2018-06-27 12:03	2018-07-04 14:08	7	1.0	556403
Nr. 25	2018-07-04 14:44	2018-07-19 10:08	15	3.6	1261023
Nr. 26	2018-07-23 12:39	2018-08-10 10:15	18	2.0	1141642

4.1.5. Turbidity measurement

Online turbidity logger at Ubstadt Gauge has detected turbidity values at a frequency of 10 minutes since 05th of June 2018. The period of time till 10th of August, which also covered the LVS operation events from Nr. 22 to Nr. 26, was the main focus. Turbidity ranged between 8 a.u. (14th of June 2018) and 8192 a.u. (22nd of July 2018). Consistent with the manually sampling time, corresponding turbidity records were combined with SSCs obtained from grabbed samples for the construction of a site-specific regression model. Negative detections, however, kept occurring since 20th of August, which implied that turbidity loggers stood a good chance of creating errors. DO and temperature in the

river were simultaneously measured and they all represented the temporary characteristics of the site where samples were collected.

5. Results and Discussion

5.1. Regression models

5.1.1. TSS model

The red, blue and purple solid lines fit with the Qmax_h (m^3/s) and TSS flux (g/s) by means of conditional exponential, linear and logarithmic models respectively. Linear* model was modified from the original linear model by getting rid of two large outliers for a better goodness of fit, but its application got narrowed on the other hand. Rating curves were likewise constructed by applying a linear regression to logarithmic flow rates and SSCs. It was obvious that SSC always leveled up as the discharge increased.

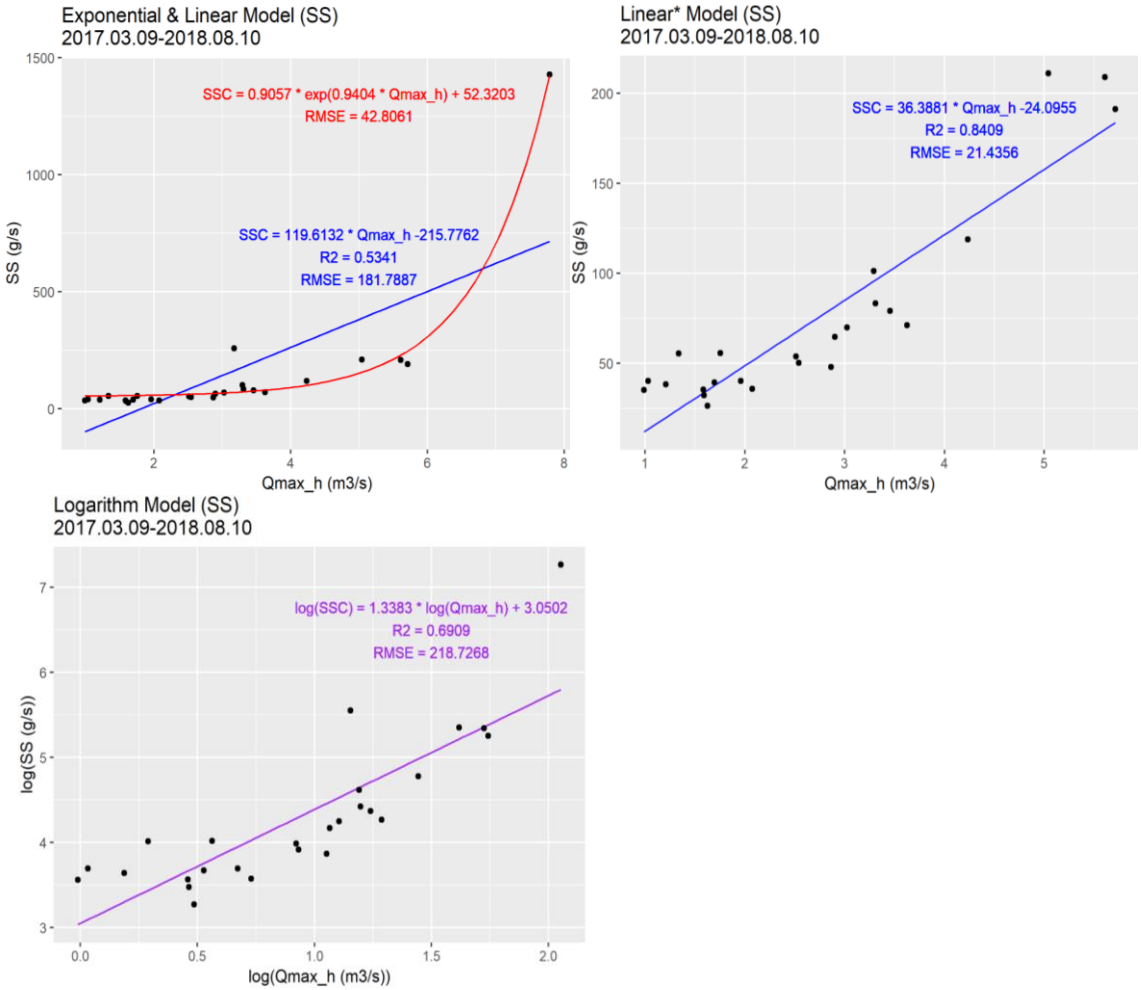

Figure 5.1 LVS-based (exponential, linear, linear* and logarithmic) rating curves for TSS

5.1.2. Nitrogen model

Total, particulate and dissolved nitrogen were separately modeled. N_part flux displayed an analogous exponentially increasing trend as TSS, while N_dis and TN concentrations followed similar hyperbolic and linear patterns and maintained close amounts all the time, which suggested that soluble phase dominated the overall nitrogen. Modified linear models were developed on the side. Inverse tendencies existed between N_part and other N forms. To be exact, observed increases in N_part could be attributed to the flushing caused by higher flows, while N_dis along with TN constantly decreased with mounting flows as a result of dilution.

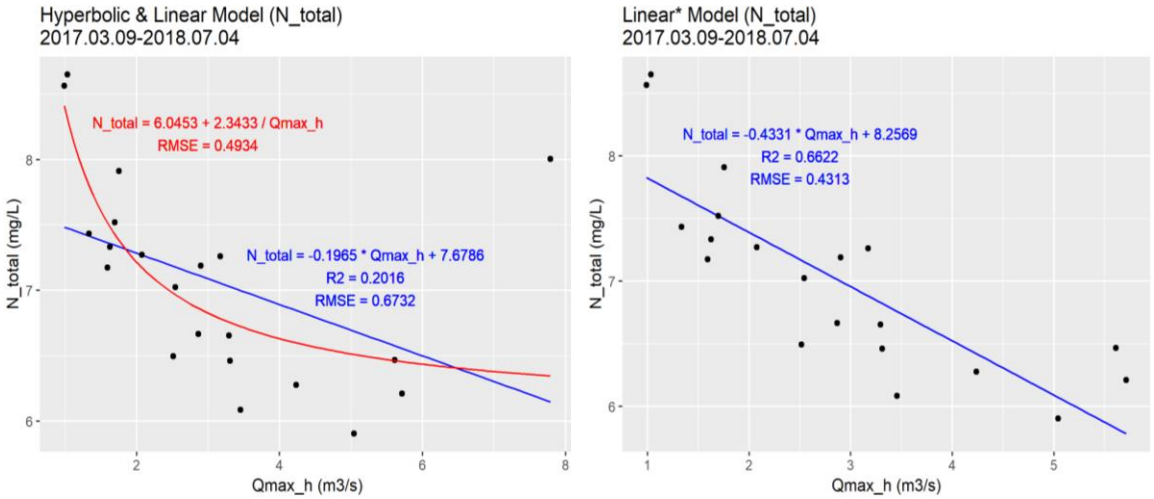

Figure 5.2 LVS-based (hyperbolic, linear and linear*) rating curves for TN

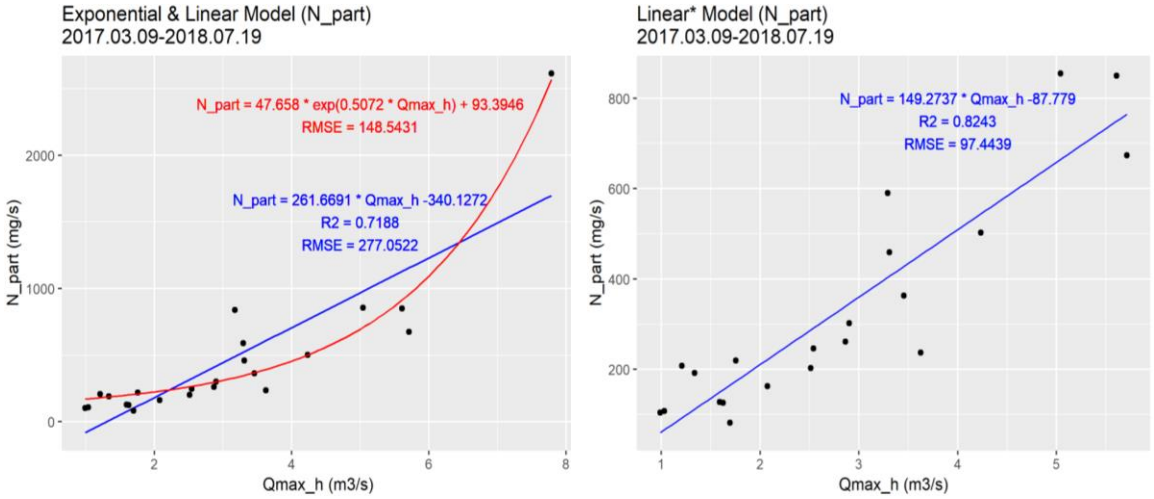

Figure 5.3 LVS-based (exponential, linear and linear*) rating curves for N_part

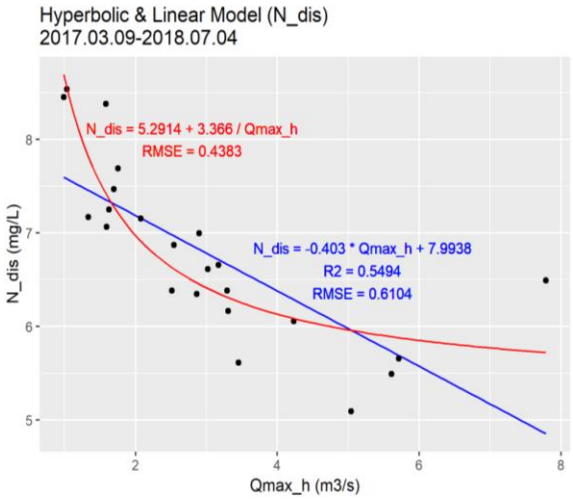

Figure 5.4 LVS-based (hyperbolic and linear) rating curves for N_dis

5.1.3. Phosphorus model

P_part, as a leading component of TP, its exponential growth pattern was almost identical to TP. Modified linear models to a certain extent improved the linearity at the cost of more restricted applicable range in these cases too. Dissolved phosphorus (P_dis) was measured but uninvolved in the regression model construction owing to the absence of noticeable relation to discharge values. Hence, its fluvial load was assumed to be the difference between TP and P_part.

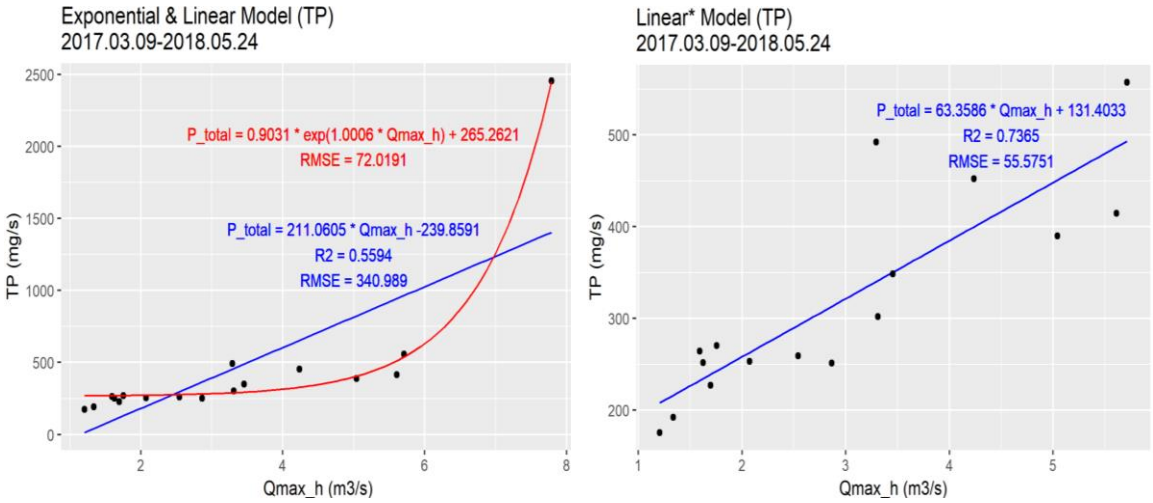

Figure 5.5 LVS-based (exponential, linear and linear*) rating curves for TP

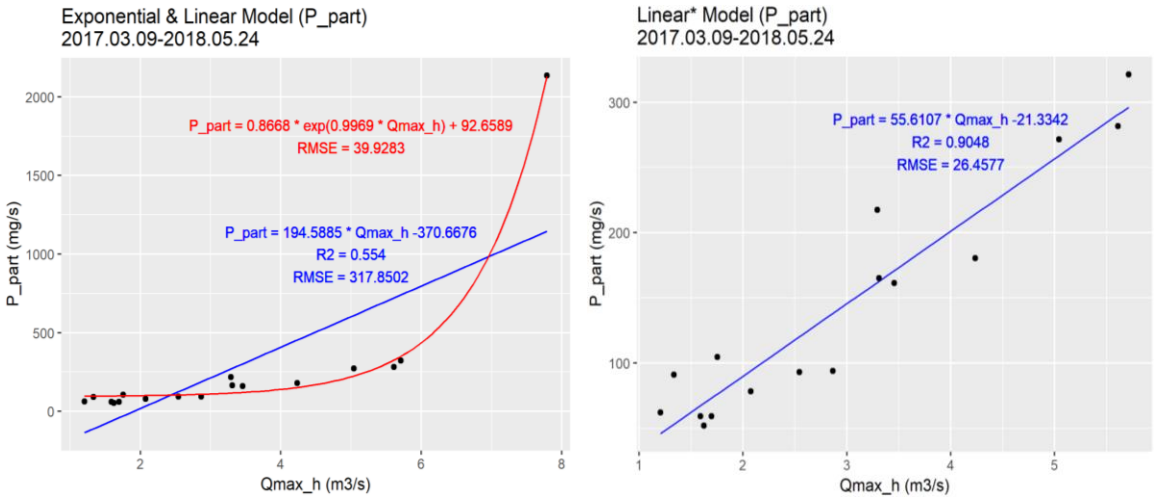

Figure 5.6 LVS-based (exponential, linear and linear*) rating curves for P_part

5.1.4. Turbidity model

As was expected, strong linearity existed between turbidity and SSC and the clarity of river water kept dropping with increasing sediment content. A close-to-one coefficient of determination made this model more convincing. Nonetheless, it concentrated on a relatively narrow turbidity range, up to 520 a.u., thus making it indeterminate to estimate in highly turbid conditions. Temperature (°C) and DO in the river were not surprisingly negative correlated. Judging by the minimum DO content, it is safe to say that Kraichbach remained in an oxygen-rich and unpolluted situation.

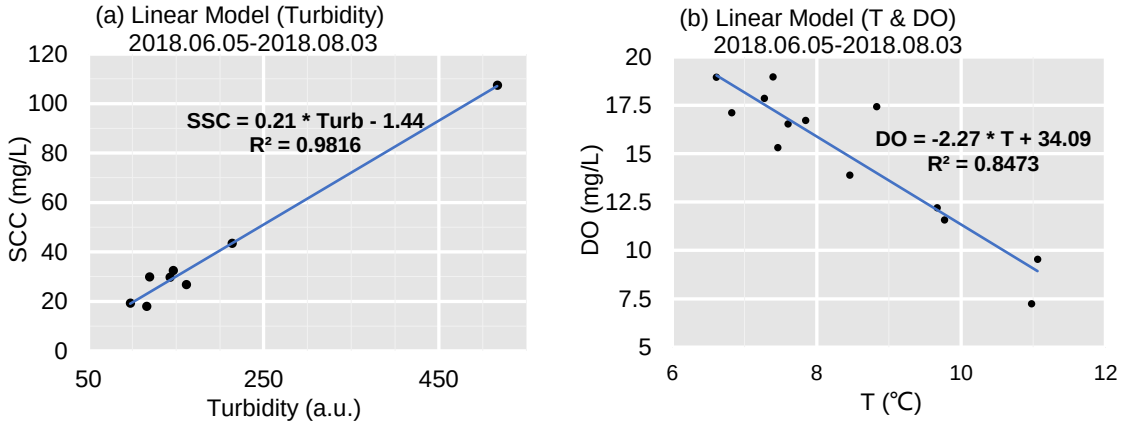

Figure 5.7 Linear regression models (a) between turbidity and SSC and (b) between temperature and DO in Kraichbach

5.1.5. Determination of optimal models

As far as TSS, N_part, P_part and TP were concerned, the exponential model exceeded the rest in consideration of smaller normalized RMSE*. Besides, in order to minimize the

level of extrapolation outside the limits of the generated rating curves, the exponential model attempted to reach towards the extremes of both discharge and concentration (flux), particularly at the upper end of the rating curve (Harrington and Harrington 2013, p. 31). Resultant negative concentration estimates by linear models when discharge values tended to be infinite small made it more illogical than exponential ones. For instance, the linear model produced negative sediment loads even down to -1984 t/a (Figure 5.8) and several negative particulate phosphorus fluxes (Figure 5.10) in 1976-2015. Negative estimates did not show up in 2017/2018 for either parameter.

During the years 1976-2015, the predicted masses of N_dis by linear and hyperbolic models were nearly the same, averagely 0.2% deviation. However, the linear model was selected over the other one in spite of its higher RMSE*, since the hyperbolic model predicted a constant concentration of 5.3 mg/L for discharges greater than 6 m^3/s. Regarding TN, a modified linear model was preferred considering its larger coefficient of determination R^2 and smaller RMSE*, even though its estimation ability was still quite unsatisfying. Likewise, the applicable range deserved attention.

Table 5.1 Comparison of models. "-" means not available; Exp., Lin., Lin*, Log., Hyp. stand for exponential, linear, modified linear, logarithmic and hyperbolic models respectively; Optimal models are highlighted in boldface.

Parameter	Model	N	Qmin	Qmax	Qmean	Qmedian	R^2	RMSE*
TSS (g/s)	**Exp.**	**26**	**1.0**	**7.8**	**2.9**	**2.7**	**-**	**0.03**
	Lin.	26	1.0	7.8	2.9	2.7	0.53	0.13
	Lin*	24	1.0	5.7	2.7	2.5	0.84	0.12
	Log.	26	1.0	7.8	2.9	2.7	0.69	0.16
N_dis (mg/L)	Hyp.	23	1.0	7.8	3.0	2.9	-	0.13
	Lin.	**23**	**1.0**	**7.8**	**3.0**	**2.9**	**0.55**	**0.18**
N_part (mg/s)	**Exp.**	**23**	**1.0**	**7.8**	**3.0**	**2.9**	**-**	**0.06**
	Lin.	23	1.0	7.8	3.0	2.9	0.72	0.11
	Lin*	21	1.0	5.7	2.8	2.5	0.82	0.13
TN (mg/L)	Hyp.	21	1.0	7.8	3.1	2.9	-	0.18
	Lin.	21	1.0	7.8	3.1	2.9	0.20	0.25
	Lin*	**20**	**1.0**	**5.7**	**2.8**	**2.5**	**0.66**	**0.16**
P_part (mg/s)	**Exp.**	**17**	**1.0**	**7.8**	**3.2**	**2.9**	**-**	**0.02**
	Lin.	17	1.0	7.8	3.2	2.9	0.55	0.15
	Lin*	16	1.2	5.7	3.0	2.7	0.91	0.10
TP (mg/s)	**Exp.**	**17**	**1.0**	**7.8**	**3.2**	**2.9**	**-**	**0.03**
	Lin.	17	1.0	7.8	3.2	2.9	0.56	0.15
	Lin*	16	1.2	5.7	3.0	2.7	0.74	0.15

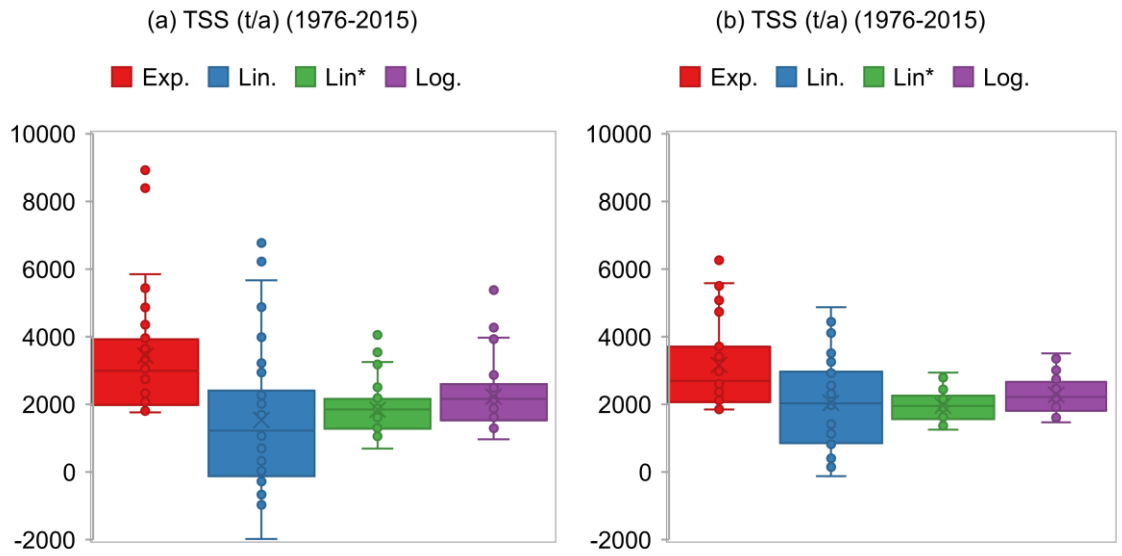

Figure 5.8 Box plots of annual TSS loads in 1976-2015 by four LVS-based models via (a) T-split and (b) V-split

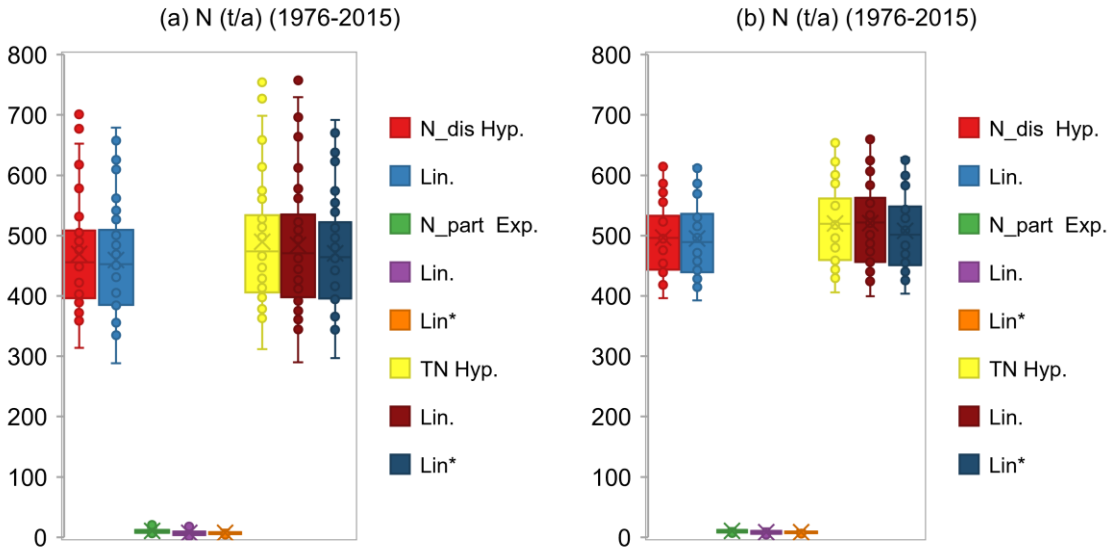

Figure 5.9 Box plots of annual nitrogen species loads in 1976-2015 by various LVS-based models via (a) T-split and (b) V-split

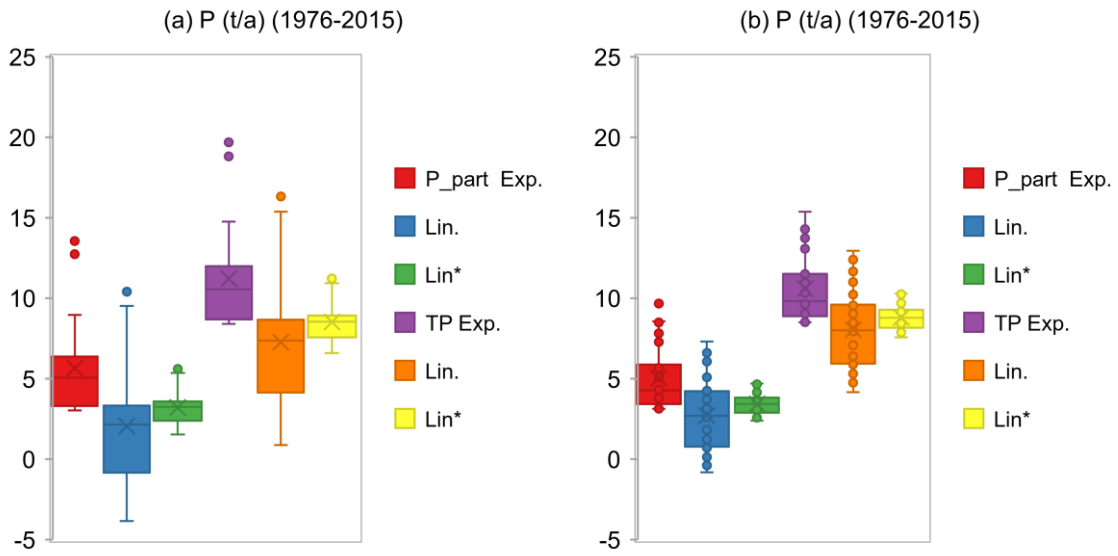

Figure 5.10 Box plots of annual phosphorus species loads in 1976-2015 by various LVS-based models via (a) T-split and (b) V-split

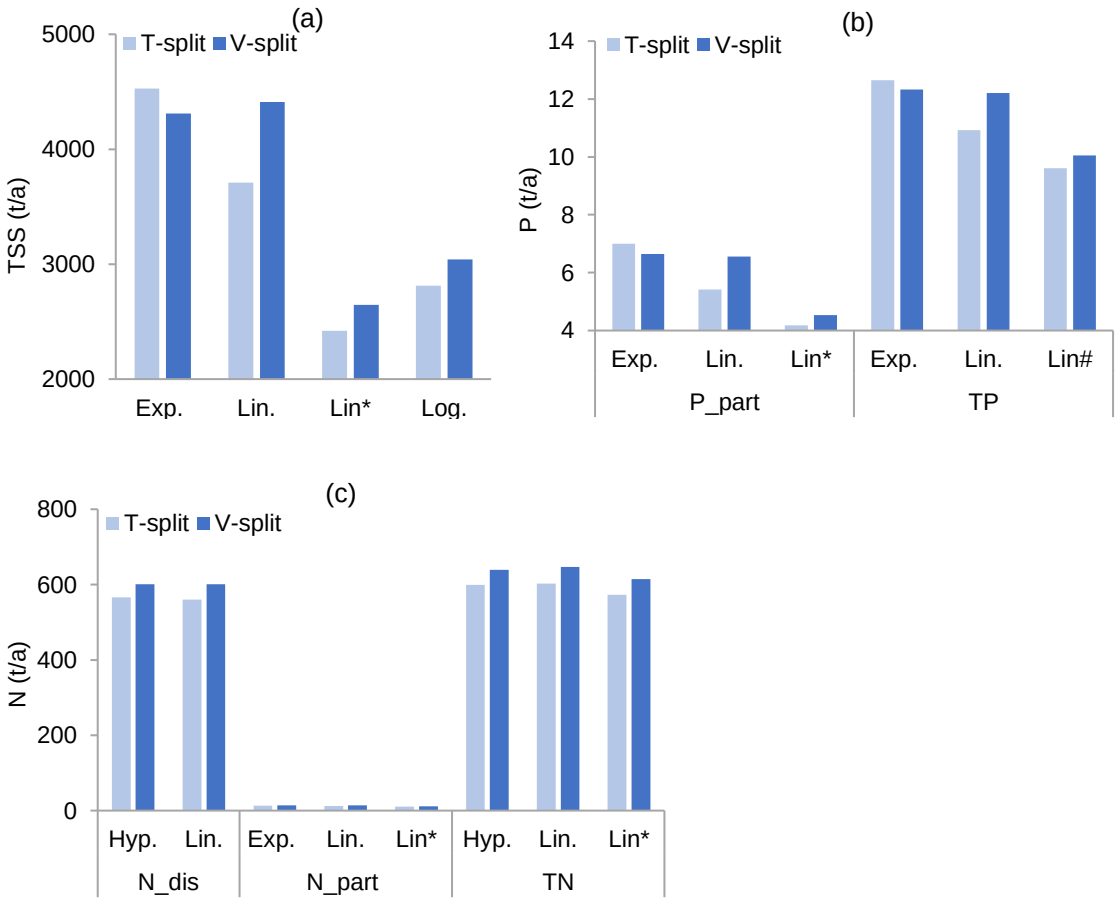

Figure 5.11 Annual load of (a) TSS, (b) phosphorus species and (c) nitrogen species for the year 2017/2018 by various LVS-based models via T-split and V-split

5.2. Fluvial loads estimation

5.2.1. Results from LVS-based models in 1976-2015

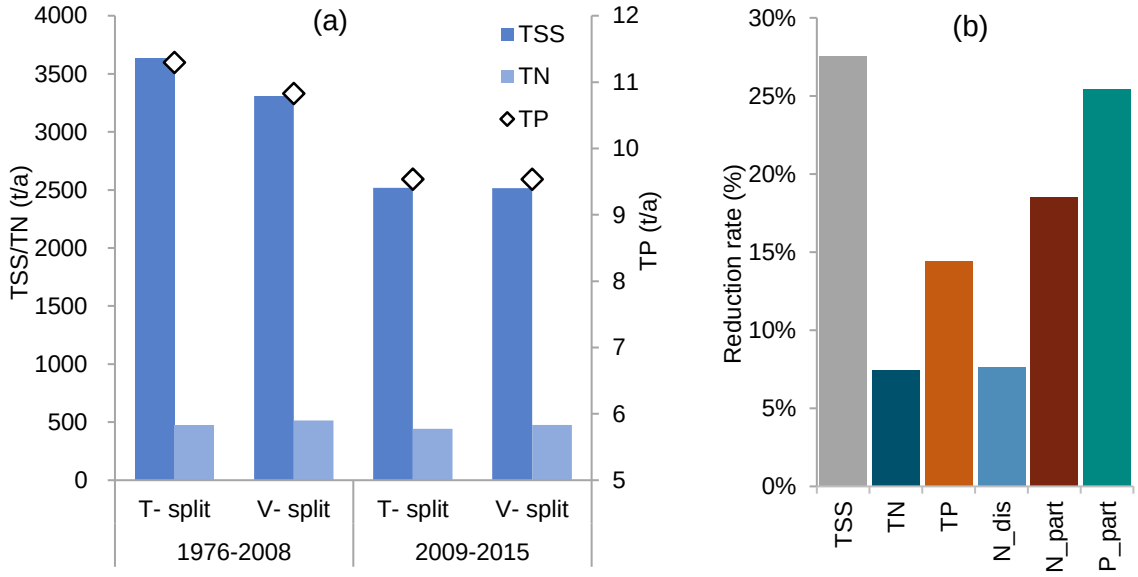

Figure 5.12 (a) Mean annual loads of TSS, TN and TP for separate time frames in 1976-2015 via T-split and V-split; (b) Reduction rate (%) of the mean annual load of TSS, N, P species after the year 2009.

The 40-year period of time was divided into two main parts, years 1976-2008, when the hydrogeological status of the Kraichbach catchment was unclear, and years 2009-2015, in which erosion reduction measures were finished and yearly emission model results were available.

Assume an unchanged hydro-geological status of Kraichbach, no matter sediment or nutrient budgets, they experienced varying levels of decline synchronously, with 28% reduction rate for TSS, 14%, 8% for TP and TN respectively. Before the year 2009, averagely seven times more TSS have been transported annually than TN, and the mean ratio of delivered TSS and TP was 299, whereas these ratios decreased in the later seven years except for an improved budget ratio between TN and TP. Compounded with reduction rate analysis as shown in Figure 5.12 (b), it can be said that transportable sediment and phosphorus were more intensively reduced than nitrogen, and particulates i.e. P_part, N_part were more significantly reduced than dissolved ones.

1) TSS, TN and TP

In terms of TSS (Figure 5.13), the annual yield fluctuated between 1767 t/a (in 1991) to 8928 t/a (in 1982) with T-split, while with V-split it varied between 1846 t/a (in 1991) to 6264 t/a (in 1985). Take an insight into the overall results, estimates based on T-split,

with a relative standard deviation (RSD) of 0.5, presented to be more fluctuating. They followed the essentially identical pattern as the original flow rate variation, which also showed three tremendous peaks. Whereas, estimates by V-split tended to be less unstable (with RSD of 0.4). They slightly outnumbered the outcomes from T-split in base flow condition years but remained less reactive to flood years like 1982, 1988 and 2002. Therefore, the overall mean annual sediment yield by V-split stayed at a lower level.

Annual TN ranged from 297 t/a (in 1991) to 692 t/a (in 1988) with T-split, with V-split ranging between 404 t/a (in 1991) and 629 t/a (in 1988) (Figure 5.14). RSDs for annual TN loads derived from both approaches were less than 0.2. The majority of predicted TN by V-split were to different degrees higher than those by T-split, particularly under low flow circumstances. In the meantime, T-split overestimated several times during storm years.

TP varied from 9 t/a (in 1991) to 20 t/a (in 1982 via T-split) and 15 t/a (in 1985 via V-split) (Figure 5.15). The coordination level of annual TP estimates via two strategies during the 40 years was in a similar manner as TSS yields. Specifically, two approaches generated similar amounts of TP in most cases but differed in wet years when T-split kept overestimating. However, the deviation of total TP results stayed at the lowest level, with averagely 0.2 as RSD.

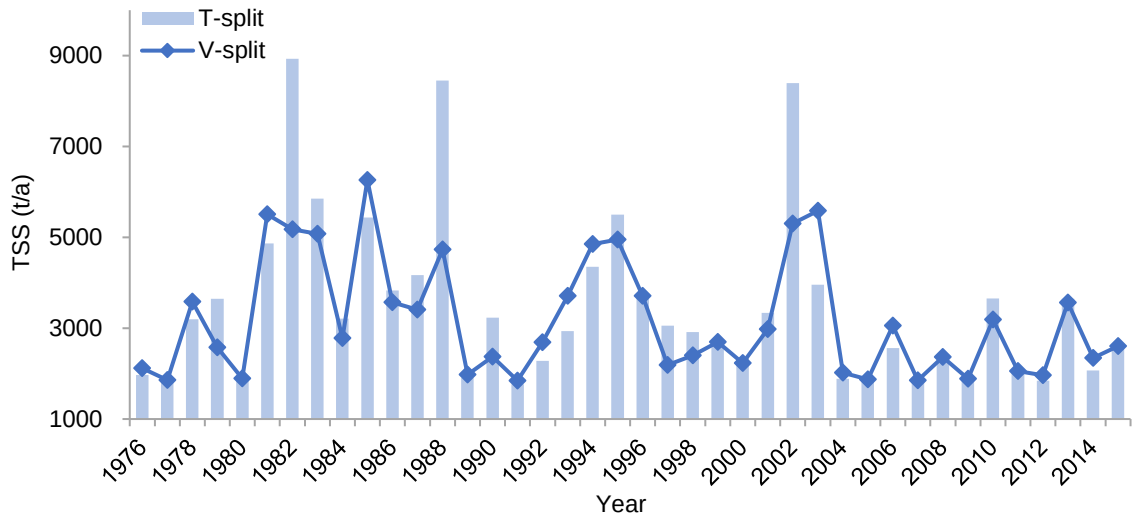

Figure 5.13 Annual TSS loads in 1976-2015 via T-split and V-split

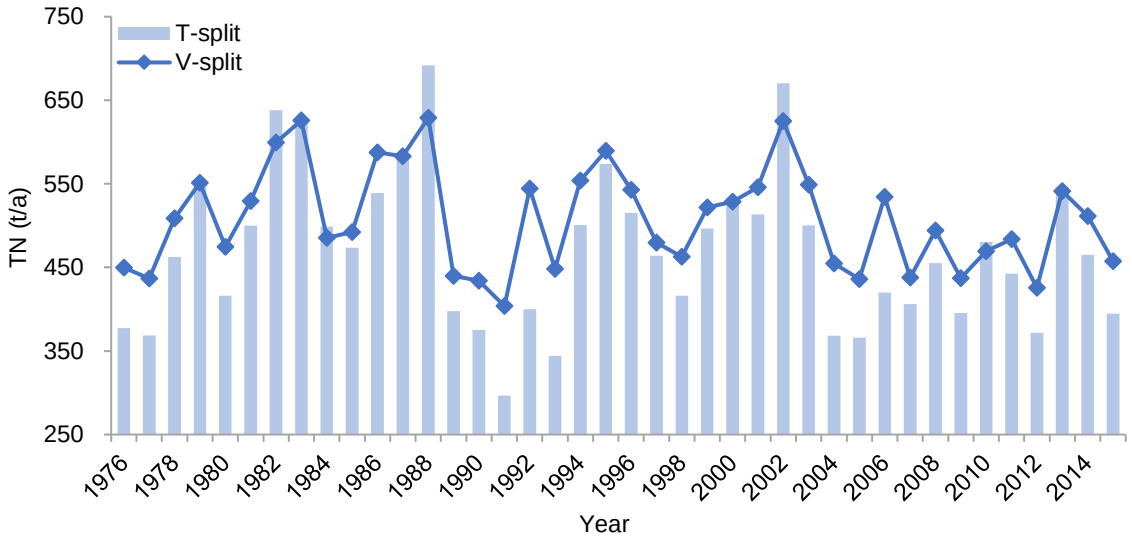

Figure 5.14 Annual TN loads in 1976-2015 via T-split and V-split

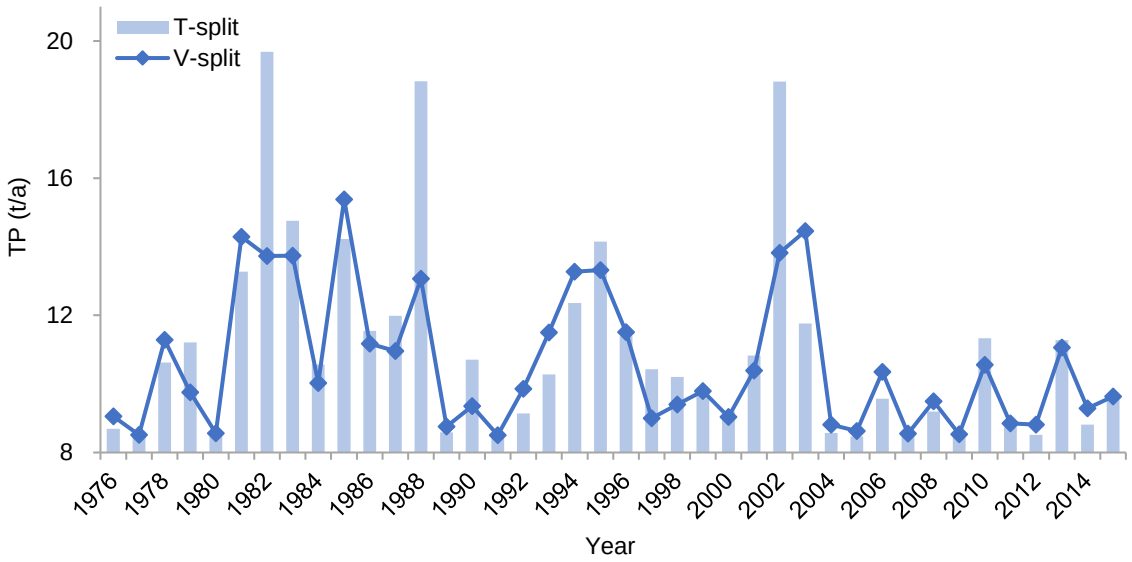

Figure 5.15 Annual TP loads in 1976-2015 via T-split and V-split

2) Dissolved/particulate N and P

Annual dissolved and particulate nitrogen fluxes were compared (Figure 5.16). The soluble phase was by both approaches the overwhelming majority, 48 times more than the insoluble phase. N_part loads based on T-split, with RSD of 0.4, altered the most dramatically from year to year. Nonetheless, both approaches and both types of nitrogen had the synchronous tendency to reach the peak and bottom, in 1988 and in 1991 respectively.

As illustrated by Figure 5.17, P_part accounted for around half of TP and the share always reduced in drought years but gained in wet years. Similarly, estimates in both

ways differ moderately only except during wet periods. Soluble phosphorus annual flux was not predictable with available datasets but was capable of being deduced as the difference between TP and P_part.

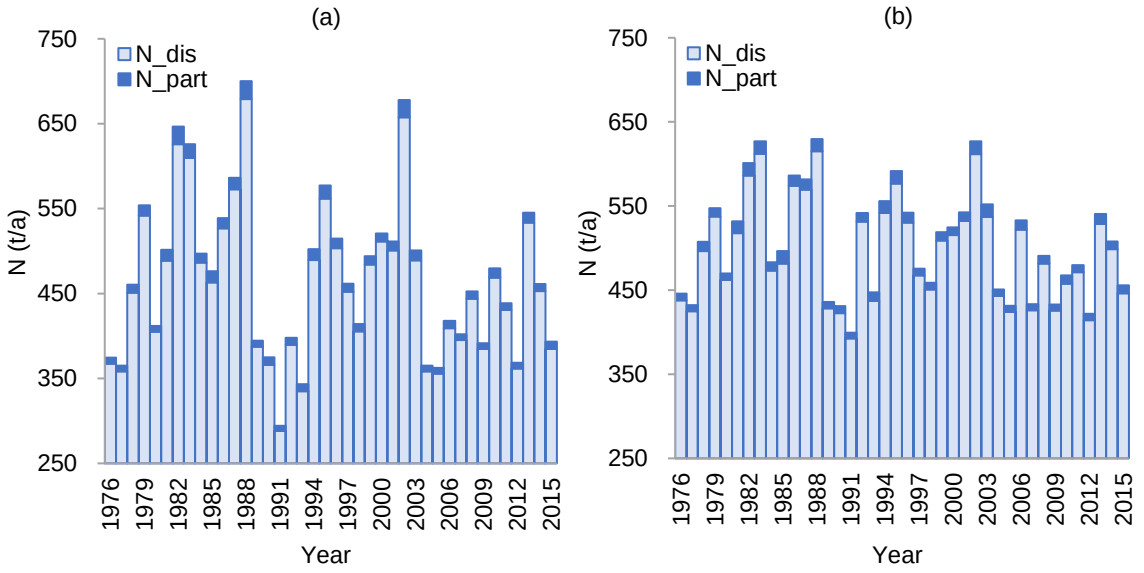

Figure 5.16 Annual N_dis and N_part loads in 1976-2015 via (a) T-split and (b) V-split

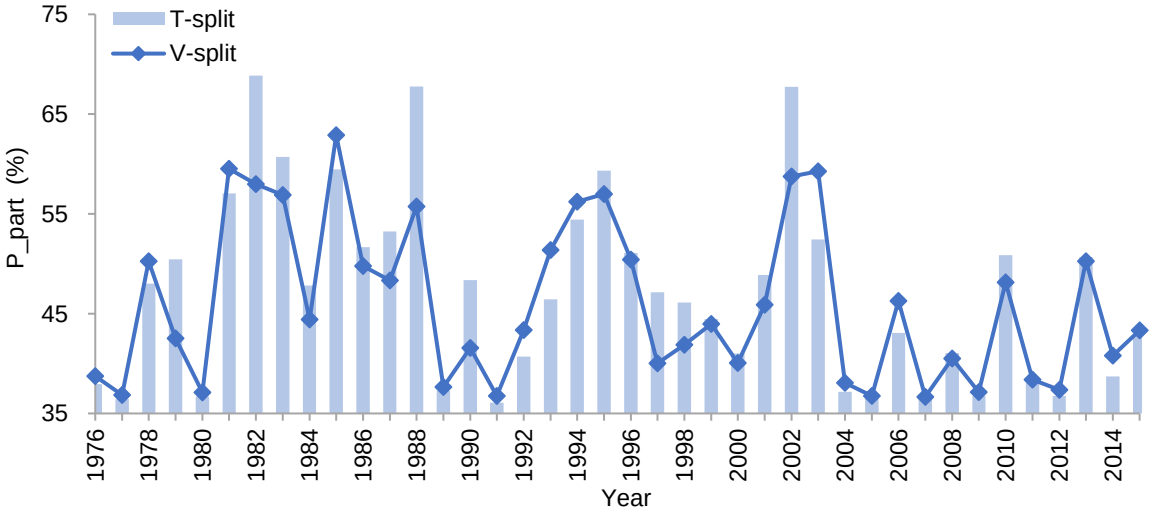

Figure 5.17 Annual mass share of P_part (%) in 1976-2015 via T-split and V-split

3) Comparison with MoRE model

During the six years from 2009 to 2014, apparently, LVS-based approaches appraised masses were almost continuously greater than those quantified by MoRE system according to Figure 5.18, even if their variation tendencies stayed comparable. In greater detail, the mean ratios of LVS-based and MoRE modeled nutrient budgets were 2.1, 1.6 and 1.5 for TN, TP and PO_4-P respectively.

In the light of MoRE model, on average 6 t phosphorus including 4 t reactive phosphates and 237 t nitrogen were released into Kraichbach annually. Years 2010 and 2013, as relatively more pluvial periods of time, unquestionably contributed more. 39 times more nitrogen than phosphorus migrated in the river, and this value ascended in high flow year 2013. Soluble phosphorus represented persistently 65% of TP regardless of flow conditions.

Taking an in-depth insight into the emission sources, groundwater occupied roughly 55% of overall TN release, followed by interflow at the upper level of groundwater (22%) and WWTP effluent (18%). Surface runoff (3%) and other sources (2%) played less important roles in the contribution of nitrogen. Apart from the nearly constant influences of WWTP and erosion on TN, other pollutant sources always varied with the same pace at their own levels.

As for TP and phosphate species, WWTP was viewed as the most essential pathway, accounting for 50% and 56% of total emissions. Less importantly, surface runoff emitted 19% and 29% of TP and PO_4-P into the river. The difference was, erosion caused 18% of TP yields but imparted nothing to dissolved phosphorus species. In contrast, another major source for PO_4-P was urban systems, where combined or separate sewer overflows made contributions. For chosen parameters, only erosion effects sustained at the identical level, while the impacts of WWTP and other pathways kept almost synchronous variation.

With one accord, all the water parameters of interest were hardly impacted by industrial wastewater effluent.

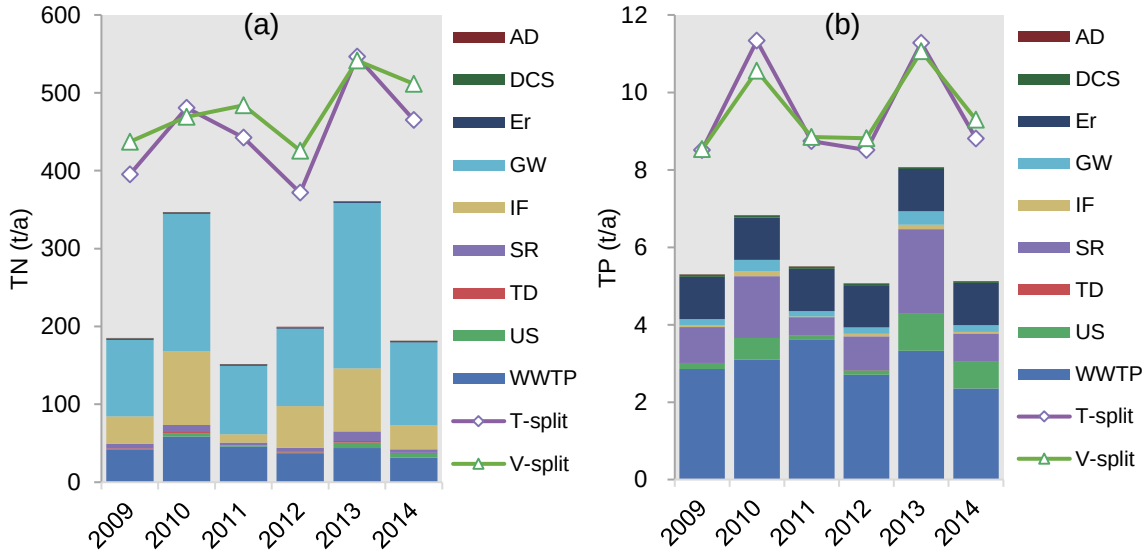

Figure 5.18 Emission fluxes of (a) TN, (b) TP and (c) PO_4-P via various pathways in 2009-2014 according to MoRE model (source of data: IWG-SWW 2018).

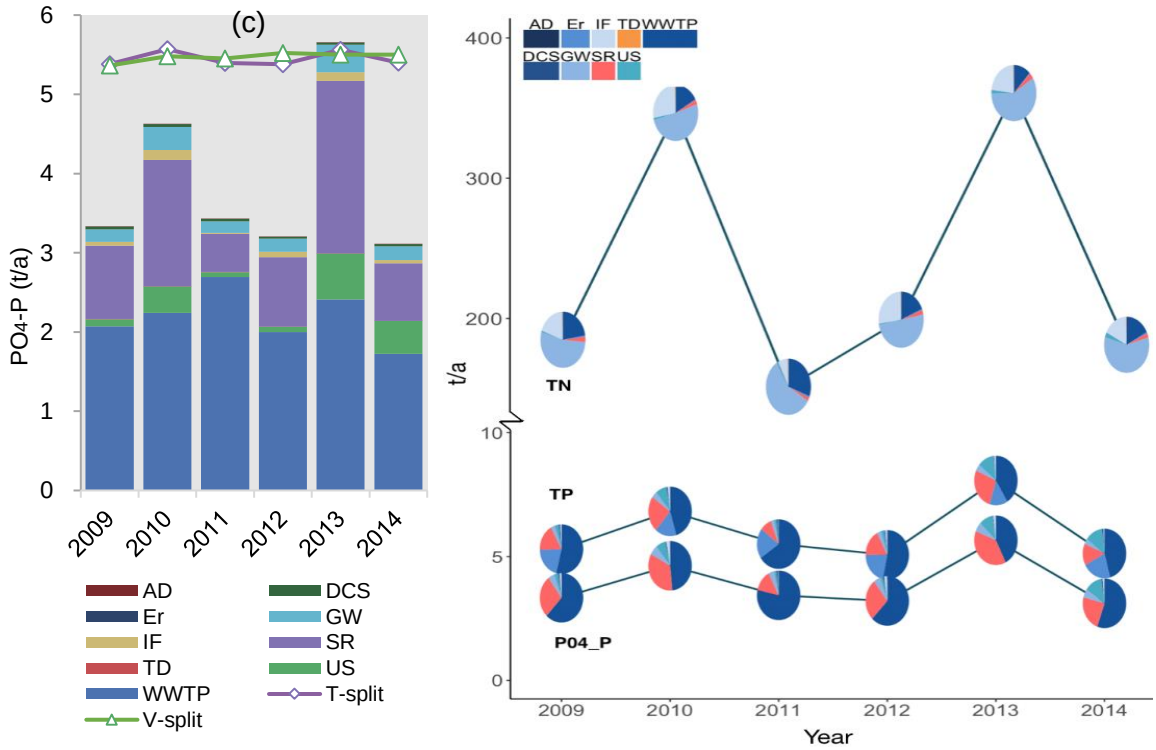

Figure 5.19 The contribution trend of various pathways to the annual load of TN, TP and PO_4-P in 2009-2014 according to MoRE model (source of data: IWG-SWW 2018).

5.2.2. Hilden approach in 2017/2108

One year lasting since the July of 2017 was designated to compare the annual fluxes based on Hilden approach and LVS-based models.

Because of constrained grab sample measurements, Hilden approach was limited to the calculation of TSS, TP, P_part, P_dis and N_dis which consisted of NH_4-N, NO_3-N and NO_2-N, but insoluble and total nitrogen remained unknown. Taken as a whole, traditional Hilden approach remarkably underpredicted all the water quality parameters in comparison to LVS-based approach. Particularly for TSS, estimates by means of T- and V-split were more than 3-fold of that by Hilden calculation. As regards other parameters, the ratio numbers were all approximately 2.

However, after redefining the correction factor, the adjusted Hilden approach produced nearly the same results as those by the LVS-based approach. Relevant p values for involved parameters are listed in Table 5.2. Taking TSS as an example, the mean value of the highest 2% discharges, rather than the overall mean flow rate, was used in Equation 6 to generate a corrected load. This adjusted version of Hilden approach called for additional monitoring practices, and it emphasized the importance of involving peak events into fluvial load estimation. However, its extrapolation to other catchments or other timeframes might be problematic, because watershed condition and hydrological status can be quite different.

It was found that NO_3-N dominated over other soluble nitrogen species by representing 93% of total N_dis, NH_4-N (4%) and NO_2-N (3%) were certainly in the minority. There was a preponderance of dissolved species (64%) in TP in accordance with Hilden.

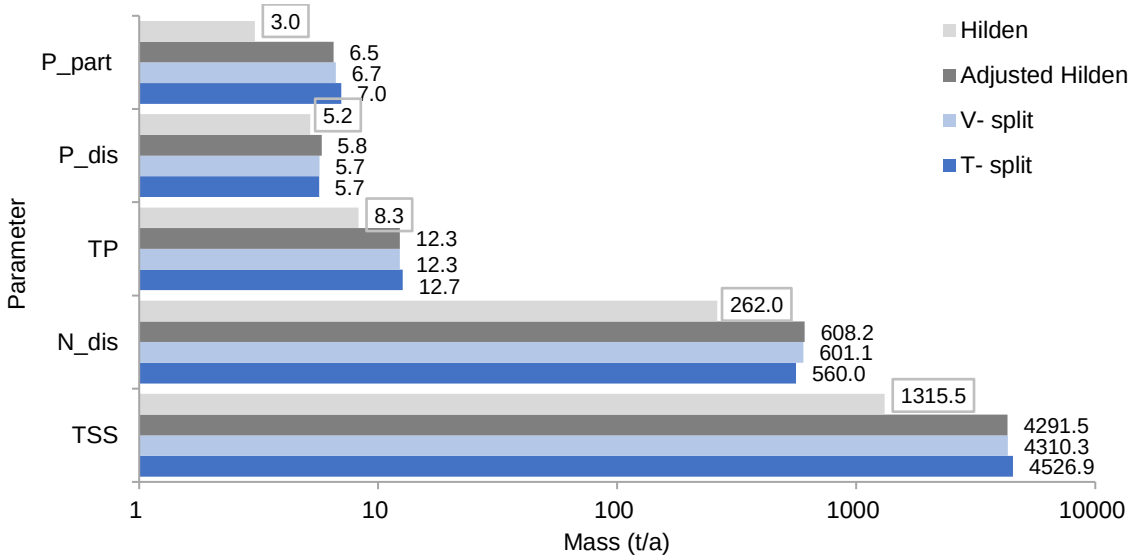

Figure 5.20 Annual TSS loads for the year 2017/2018 via Hilden, adjusted Hilden, T-split and V-split

Table 5.2 Adjusting factors p (%) for the modified Hilden approach

TSS	N_dis	TP	PO_4-P
2	7	36	85

5.2.3. Feasibility study of the turbidity-based approach

In order to test the practicability of using turbidity as a proxy to predict sediment load, the period of time that covered the last five LVS operation runs was investigated. The up limits detected for turbidity and discharge value were 4000 a.u. and 4 m^3/s respectively.

For the two months as a whole, the turbidity-based method worked out in all 248 t transported sediment, 26% less than by means of LVS-based approaches.

Combing Figure 5.21 and Figure 5.22 (a), during event Nr. 22, flow rate frequently peaked around 2.5 m^3/s, but turbidity device merely responded once to the turbulence, thus giving rise to a more than 300% underestimation, in comparison to LVS result. Afterward, gauging station continuously recorded two low flow events, when discharge values maintained around 1 m^3/s. Turbidity sensor aligned itself with flow condition in event Nr. 23 by revealing high clarity of water body but still kept an around 300% underestimation. For unobvious reasons turbidity consecutively stayed at slightly high

levels in Nr. 24, thus leading to 61% more prediction of sediment. Event Nr. 25 lasted a relatively long period of time, in which two discharge peaks showed up, accompanied by only one unsatisfactory turbidity response. Event Nr. 26 missed the chance to cover a flood on 22. July, but later caught two insignificant peaks, one of which was somewhat reflected by the turbidity sensor. Last two events again estimated less than LVS measurements by 40%-58%.

So, the turbidity-based approach had the tendency to predict less amount of TSS in most of our cases. In particular, during continuous high or low flow conditions, the degree of underestimation was more momentous. In rare circumstances, turbidity-based results were also probable to overestimate or create error signals, possibly due to a block of optical device window by leaves, local turbulence caused by aquatic creatures or device errors. No linear or any other regression models fit the relationship between the results from these two approaches (Figure 5.22 (b)), thereby no further interpretation was possible. All in all, despite its convenience and efficacy, turbidity-based model suffered from a major drawback: great underestimation in the case of Kraichbach.

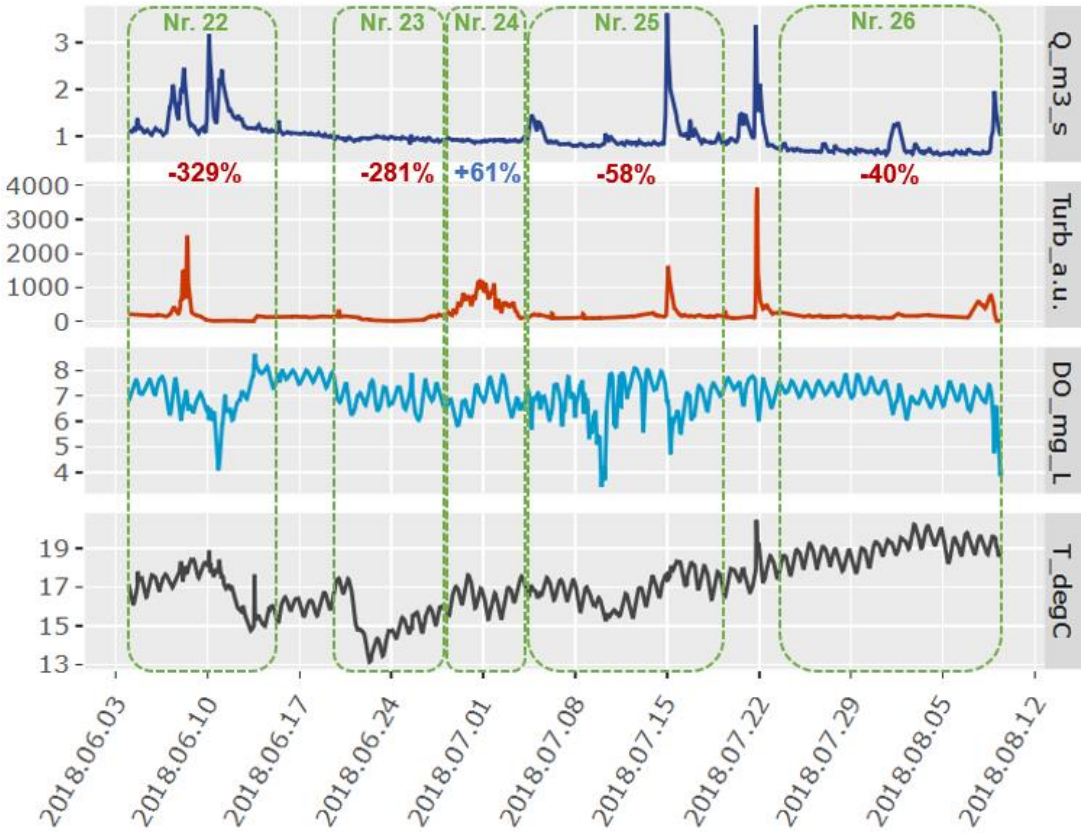

Figure 5.21 Measurements of flow rates (Q_m3_s), turbidity (Turb_a.u.), dissolved oxygen (DO_mg_L) and temperature (T_degC) at the Kraichbach gauging station for the period of 2018.06.05-2018.08.10. The numbers showed the overestimation (blue) or underestimation (red) degree of turbidity-based method.

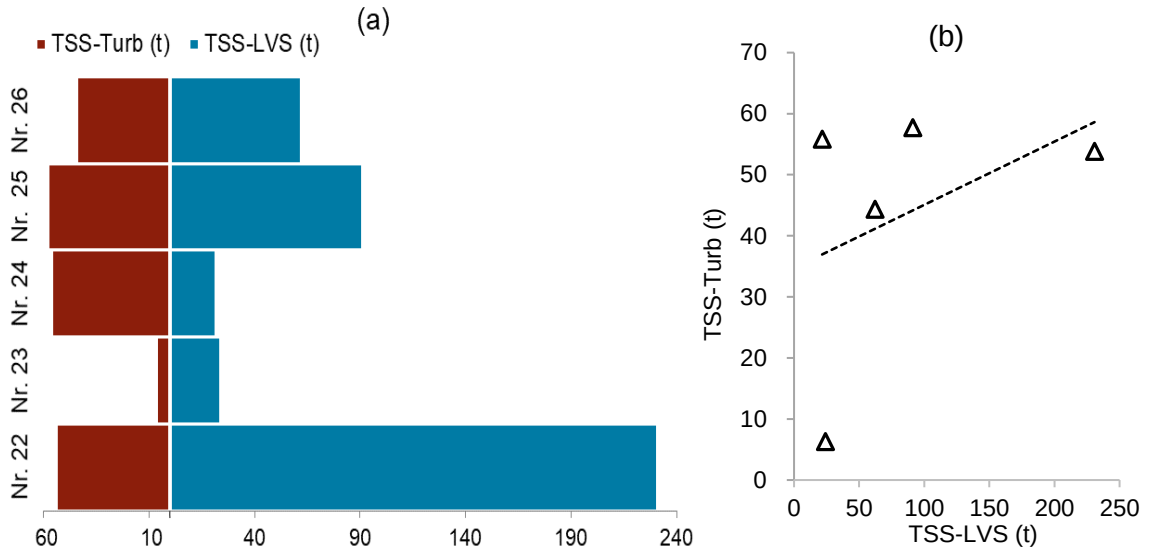

Figure 5.22 (a) Comparison of TSS loads via turbidity-based and LVS-based methods for the period 2018.06.05-2018.08.10 (which covered the last five LVS operation runs); (b) Relation between TSS loads via LVS-based and turbidity-based methods for the period 2018.06.05-2018.08.10.

5.3. Comparison between T- and V-split methods

To compare T-split and V-split methods as analytical tools to accomplish the budgeting of sediment and nutrients, annual results during years 1976-2015 were compared. As in Chapter 5.2.1 mentioned, T-split maintained slight underestimation in low and base flow years but had the tendency to overestimate in storm years.

Typically, the load ratio between T- and V-split of all parameters varied over the years with basically the same pace. As illustrated by Figure 5.23, an overestimation by T-split is expressed by a ratio larger than 1. Otherwise, either T-split estimated less or two methods predicted equal amounts of substances. For TSS and P_part, the trends of the ratio were identically pointy, reaching the top at 1.8 in the flood year 1988 and dropped to the lowest level at 0.7 in a base flow year 2003. TP and N_part were the same cases as the former pair of parameters but fluctuated less spikily, with ratios ranging between 0.8-1.5. Quite the reverse, close-to-one ratios occurred more commonly in the budget computation of dissolved and total nitrogen, implying more accordant results by way of two methods. To be more precise, linear relations between results via both methods were built for each parameter and the coefficient of determination R^2 was 0.7 for TSS and phosphorus but 0.9 for nitrogen. The estimated mass ratios for the year 2017/2018 also conformed to these rules.

Therefore, for the aim of more accurate prediction, there is no point to cope with sediment and phosphorus load by means of the T-split method, especially in pluvial

years. But it is feasible to regard T-split as a convenient alternative to estimate the annual nitrogen quantity transported in the river, particularly the dissolved form.

Nonetheless, the fact that V-split tented to be less reactive to flood years like 2002, instead it peaked in a medium flow year 1985, aroused concerns about the validity of LVS-based model. Since rating curves in exponential way were actually conditional, namely, all the discharges larger than HQ_2 were assigned as HQ_2.

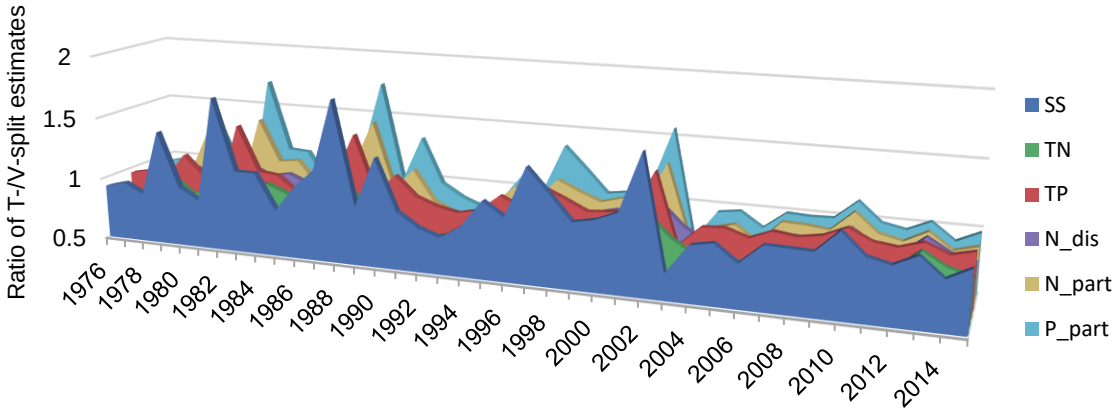

Figure 5.23 Ratio of annual loads calculated by T- and V-split in 1976-2015

5.4. The contribution of peak events

In 1976-2015, on average, 79% of the annual sediments were transported by the highest 10% of discharge percentile, and 9% of the sediment were delivered by the [Q80,Q90) discharge class. Other discharge percentiles from 0 to Q80 delivered in all 12% of the total mass. Especially for wet years such as 2002, when total transported loads were above 8000 t/a, discharge values above Q90 transferred up to 97% of them. For dry years like 1991 with less than 1900 t/a load, 27% of them were transferred by flows belonging to [Q90,Q100) class, which was still the main driver, but the other classes started to play unignorable roles. In addition, the transported mass quantity continually experienced dramatical increases with elevated flow conditions.

In 2017/2018, the dominating role of high flows played in TSS delivery is again displayed by Figure 5.26. In accompany with only two flood events characterized by close-to-HQ_2 flow rates in May 2018, 47% of overall TSS were transported. By both approaches, 85%-88% of annual TSS budgets were delivered by the [Q90,Q100) discharge percentile.

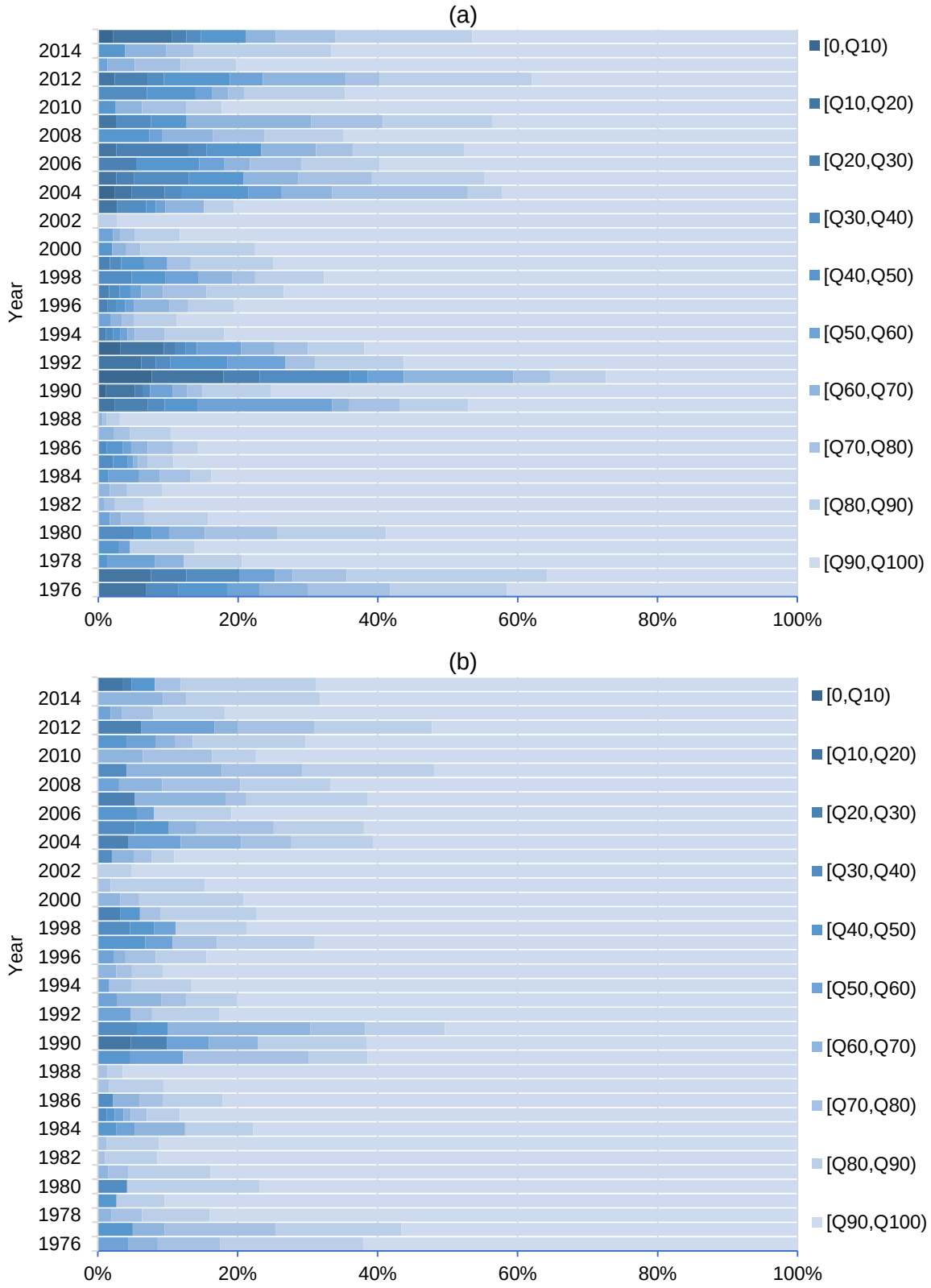

Figure 5.24 The contribution of percentile discharge classes to annual sediment load in 1976-2015 via (a) T-split and (b) V-split

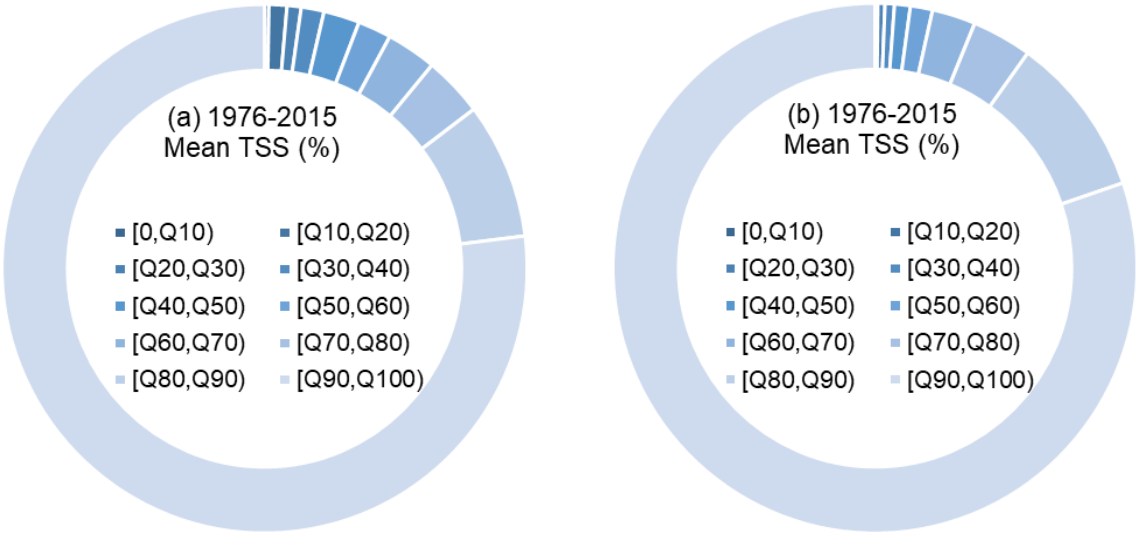

Figure 5.25 The contribution of percentile discharge classes to mean annual sediment load in 1976-2015 via (a) T-split and (b) V-split

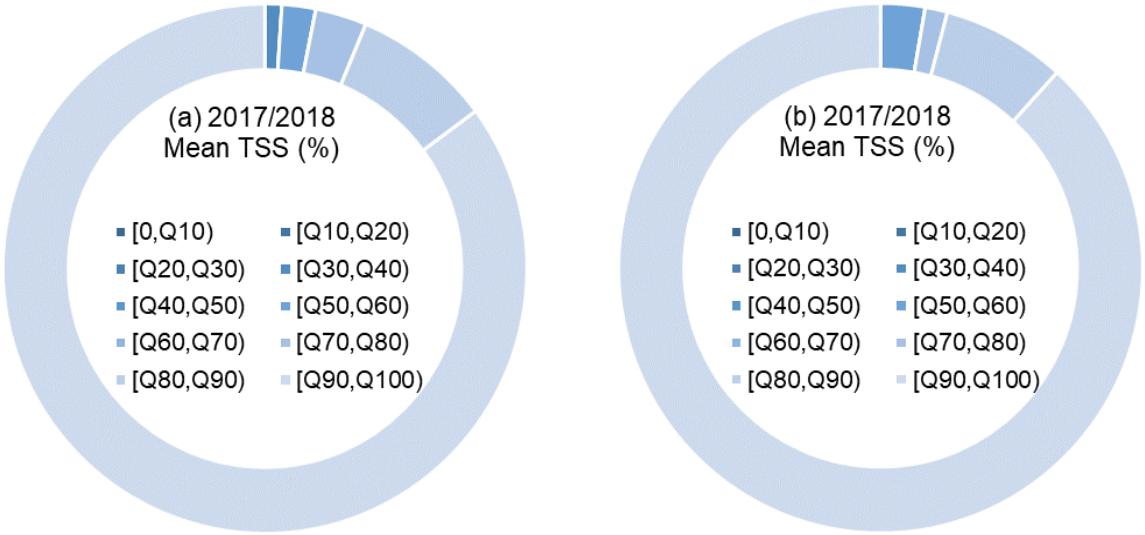

Figure 5.26 The contribution of percentile discharge classes to mean annual sediment load in 2017/2018 via (a) T-split and (b) V-split

5.5. Correlation among the annual loads of TSS, N and P

The correlation coefficients between the annual masses of each pair of parameters are indexes to highlight the possibility to predict one of them directly from the others. Basically, all the correlations kept the same ideal level as found in original flux datasets, especially by T-split. In other words, even though discharge datasets were applied to different rating curves and splitting methods, the resultant budgets of all the parameters

still maintained closely connected. This finding confirms again that the annual load was controlled directly by the total water volume in each year.

Together these Figures provide another promising budgeting approach in the future when only limited indirect data are extant. In the case of Kraichbach, by either LVS-based approach, the strongest linear relationship was believed to be present among TSS, TP, P_part and N_part, also between TN and N_dis. Visualized relations among loads of all the parameter are in detail plotted in Figure 5.27 and their internal correlation coefficients are displayed in Figure 5.28.

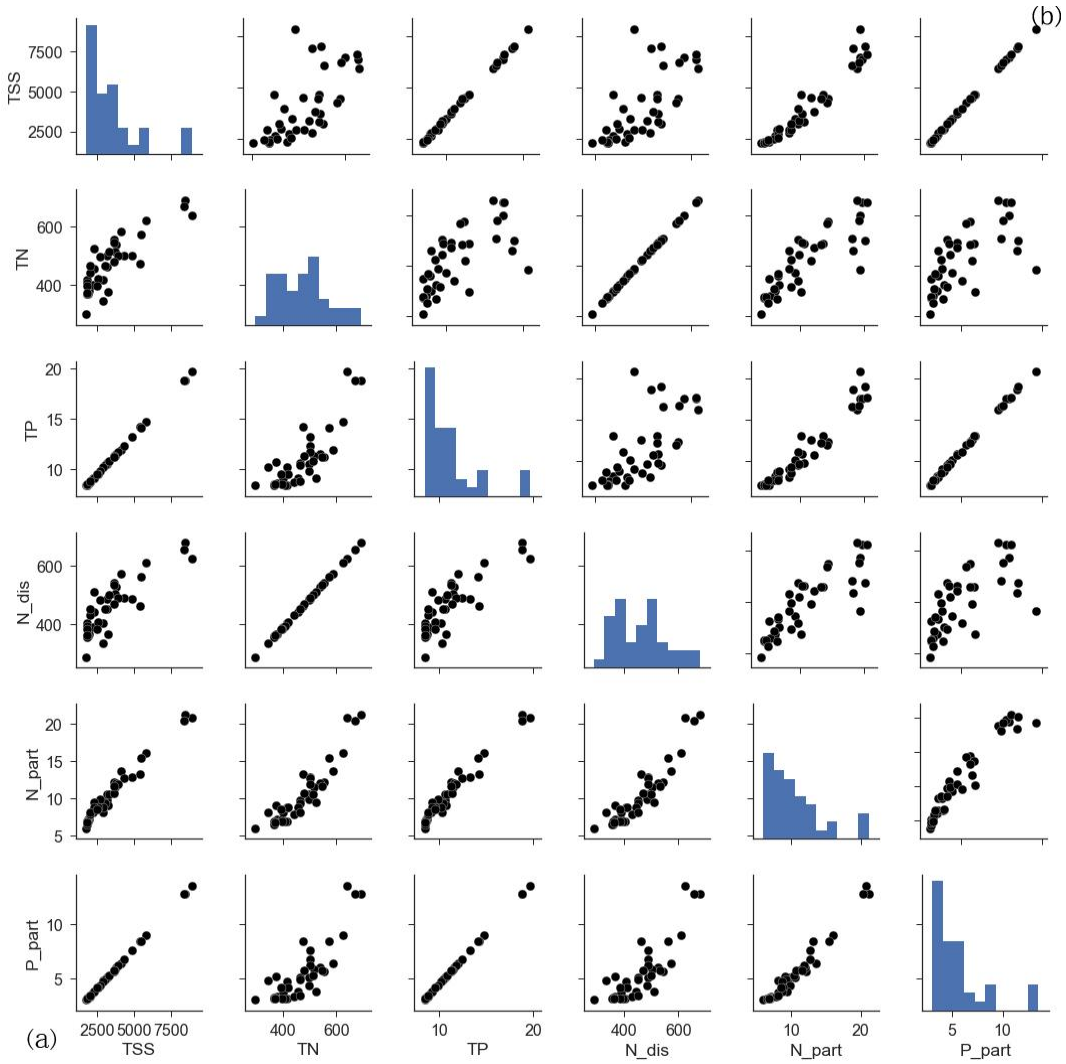

Figure 5.27 Correlation plots among the annual loads of water quality parameters in 1976-2015 via (a) T-split and (b) V-split

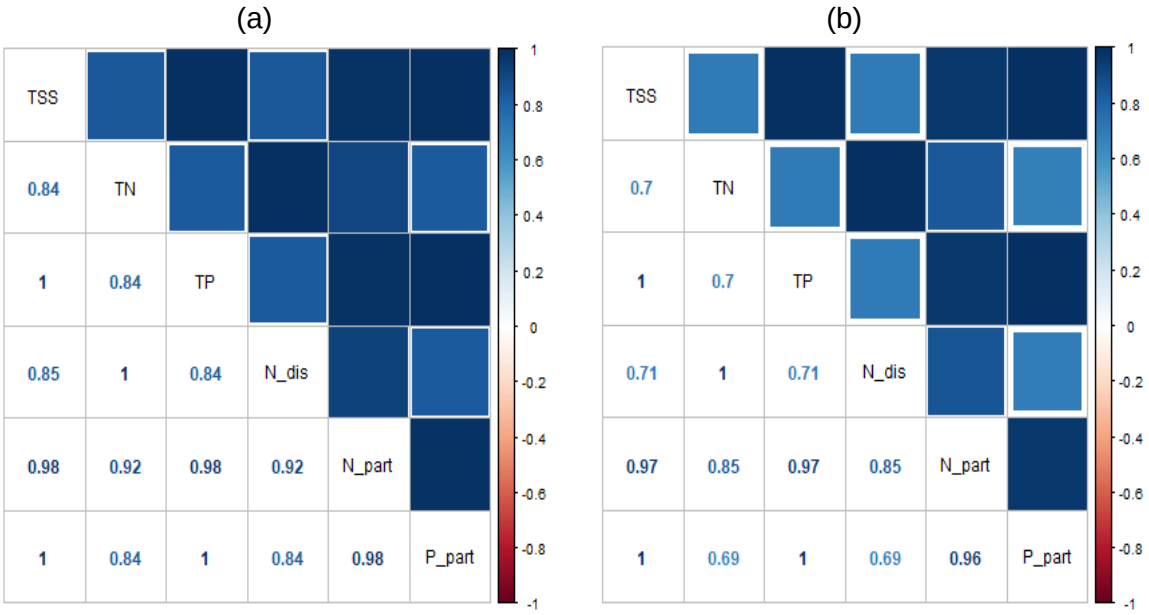

Figure 5.28 Correlation coefficients among the annual loads of water quality parameters in 1976-2015 via (a) T-split and (b) V-split

6. Watershed implementation

To promote an integrated watershed management, obtained results can be interpreted so as to guide erosion or eutrophication control measures.

Take a wet year 2002 as an example, 8392 t TSS was transported in Kraichbach (assume all the fluvial TSS originated from arable lands). Based on the mean soil bulk density (e.g. 1.1 g/cm^3) (Burghardt and Schneider 2016) and the area of agricultural lands that contribute to fluvial sediments (39 km^2) (GALF 2018) within the Kraichbach catchment, the average erosion rate can be calculated as 0.2 mm/a. Combining the erosion rate with natural soil renewal rate (0.1-0.2mm/a), the necessity or evaluation of erosion control measures can be determined. As for a medium year like 1998, the mean erosion rate is 0.06 mm/a.

As a matter of fact, the degree of erosion is quite heterogeneous within a catchment, and can also result from other sources. To be precise, notable erosion is more likely to be induced in the non-vegetated and steep areas, and grass-covered river banks are reported to be more vulnerable than tree-planted banks. Hence, targeted control plans are highly recommended.

According to LTZA (2018), the mean concentration of TP in arable lands within this catchment was 1.02 g/kg. As a result, 0.1 g/m^2 TP was in the meantime delivered into the river in 2002. With this value, the eutrophication risk can be assessed and policymakers are more likely to make wise agri-environmental decisions.

7. Conclusions and outlook

In this thesis, the fluvial load estimation of sediment and nutrients was accomplished by means of LVS-based and other quantification approaches for the Kraichbach catchment in Baden-Württemberg.

The LVS-based approach (including T- and V-split methods) was on the basis of a discharge-proportional sampling regime and highlighted the influence of high flows, therefore it was believed to produce the most accurate results. In agreement with previous studies, the hydrological condition was the most decisive factor to control fluvial budgets, the vast majority of which were therefore attributed to only a smaller number of flood events. Additionally, strong correlations were present among the annual loads of almost all the selected water quality parameters, which provided another way to budget when datasets were limited. Nonetheless, concerns have been raised due to the fact that T-split was not theoretically valid, meanwhile V-split was not sufficiently sensitive to flood years, in that applied rating curves were actually conditional.
In comparison, the turbidity-based approach suffered from remarkable underestimation, probably due to the relatively narrow application range involved in the turbidity-SSC regression model, which was basically established under low flow circumstances. Likewise, traditional Hilden approach estimated much fewer budgets of sediment and nutrients. This great bias was attributed to its dependency on infrequent grab sampling, by which high flows were considerably underrepresented. Improved performances were achieved by an adjusted version of the Hilden approach, which involved a calibration by LVS-based estimates and emphasized the determinant role of the highest p% of discharges played in fluvial budgeting. However, with current p values, the performance of this method cannot be guaranteed when it is extrapolated to other timescales or catchments, since the hydro-geological status of rivers and catchment conditions might differ. Relative to LVS-based estimates, MoRE model generated a grossly lower level of nutrients. Reasons for the deviation remained unclear at present, but riverbed erosion, erosion from urban sources, forests and meadows, and the enrichment of nutrients during transportation can be parts of them.

In further researches, a hydrology-based sampling regime is recommended for the fluvial load quantification and peak flows deserve special monitoring strategies, such as more frequent sampling in rainfall-rich or snow-melting seasons. Secondly, the extrapolation and generalization of adjusting factor p for Hilden approach to other watersheds and timeframes are of interest. Last but not least, the involvement of a broader range of flow conditions into the LVS-based models so as to more thoroughly understand the actual trends of rating curves are important.

Acknowledgment

The author is grateful for the expertise and assistance of PD Dr.-Ing. Stephan Fuchs, Dr.-Ing. Geoökol. Stephan Hilgert, M.Sc. Adrian Wagner and the IWG (Institut für Wasser und Gewässerentwicklung, Fachbereich Siedlungswasserwirtschaft und Wassergütewirtschaft).

8. Publication bibliography

2000/60/EC (2000): Water framework directive.

91/676/EEC (1991): COUNCIL DIRECTIVE (91 / 676 /EEC). Concerning the protection of waters against pollution caused by nitrates from agricultural sources.

Alexander, Richard B.; Böhlke, John Karl; Boyer, Elizabeth W.; David, Mark B.; Harvey, Judson W.; Mulholland, Patrick J. et al. (2009): Dynamic modeling of nitrogen losses in river networks unravels the coupled effects of hydrological and biogeochemical processes. In *Biogeochemistry* 93 (1-2), pp. 91–116. DOI: 10.1007/s10533-008-9274-8.

American Public Health Association (1998): Printing - Standard Methods for the Examination of Water and Wastewater.

Atieh, M.; Mehltretter, S. L.; Gharabaghi, B.; Rudra, R. (2015): Integrative neural networks model for prediction of sediment rating curve parameters for ungauged basins. In *Journal of Hydrology* 531, pp. 1095–1107. DOI: 10.1016/j.jhydrol.2015.11.008.

Berry, Walter; Rubinstein, Norman; Melzian, Brian (2003): The Biological Effects of Suspended and Bedded Sediment (SABS) in Aquatic Systems:

Best, M. A.; Wither, A. W.; Coates, S. (2007): Dissolved oxygen as a physico-chemical supporting element in the Water Framework Directive. In *Marine pollution bulletin* 55 (1-6), pp. 53–64. DOI: 10.1016/j.marpolbul.2006.08.037.

Beusen, A. H. W.; Dekkers, A. L. M.; Bouwman, A. F.; Ludwig, W.; Harrison, J. (2005): Estimation of global river transport of sediments and associated particulate C, N, and P. In *Global Biogeochem. Cycles* 19 (4), n/a-n/a. DOI: 10.1029/2005GB002453.

Bridge, J. S. (2003): Rivers and floodplains. Forms, processes, and sedimentary record. Oxford UK, Malden MA USA: Blackwell Pub.

Burghardt, Wolfgang; Schneider, Thomas (2016): Bulk density and content, density and stock of carbon, nitrogen and heavy metals in vegetable patches and lawns of allotments gardens in the northwestern Ruhr area, Germany. Available online at https://link.springer.com/article/10.1007/s11368-016-1553-8, checked on 12/8/2018.

Devore, Jay L. (2012): Probability and statistics for engineering and the sciences. Eighth edition. Boston MA: Brooks/Cole Cengage Learning.

European Environmental Agency (2018): Nitrogen and phosphorus in rivers. Indicator Fact Sheet.

Evans-White, M. A.; Haggard, B. E.; Scott, J. T. (2013): A review of stream nutrient criteria development in the United States. In *Journal of environmental quality* 42 (4), pp. 1002–1014. DOI: 10.2134/jeq2012.0491.

Ferreira, João G.; Andersen, Jesper H.; Borja, Angel; Bricker, Suzanne B.; Camp, Jordi; Cardoso da Silva, Margarida et al. (2011): Overview of eutrophication indicators to assess environmental status within the European Marine Strategy Framework Directive. In *Estuarine, Coastal and Shelf Science* 93 (2), pp. 117–131. DOI: 10.1016/j.ecss.2011.03.014.

Fox, Garey A.; Purvis, Rebecca A.; Penn, Chad J. (2016a): Streambanks: A net source of sediment and phosphorus to streams and rivers. In *Journal of environmental management* 181, pp. 602–614. DOI: 10.1016/j.jenvman.2016.06.071.

Fox, Garey A.; Purvis, Rebecca A.; Penn, Chad J. (2016b): Streambanks: A net source of sediment and phosphorus to streams and rivers. In *Journal of environmental management* 181, pp. 602–614. DOI: 10.1016/j.jenvman.2016.06.071.

Fuchs, Stephan; Kaiser, Maria; Kiemle, Lisa; Kittlaus, Steffen; Rothvoß, Shari; Toshovski, Snezhina et al. (2017): Modeling of Regionalized Emissions (MoRE) into Water Bodies: An Open-Source River Basin Management System. In *Water* 9 (4), p. 239. DOI: 10.3390/w9040239.

Gesellschaft für Angewandte Landschaftsforschung bR (GALF) (2018): USLE modelling based on soil loss map by Landesamt für Geologie, Rohstoffe und Bergbau. Only arable land.

Gholizadeh, Mohammad; Melesse, Assefa; Reddi, Lakshmi (2016): A Comprehensive Review on Water Quality Parameters Estimation Using Remote Sensing Techniques. In *Sensors* 16 (8), p. 1298. DOI: 10.3390/s16081298.

Girolamo, A. M. de; Pappagallo, G.; Lo Porto, A. (2015): Temporal variability of suspended sediment transport and rating curves in a Mediterranean river basin: The Celone (SE Italy). In *CATENA* 128, pp. 135–143. DOI: 10.1016/j.catena.2014.09.020.

Guan, Qingyu; Wang, Lei; Wang, Feifei; Pan, Baotian; Song, Na; Li, Fuchun; Lu, Min (2016): Phosphorus in the catchment of high sediment load river: A case of the Yellow River, China. In *The Science of the total environment* 572, pp. 660–670. DOI: 10.1016/j.scitotenv.2016.06.125.

Harrington, Sen T.; Harrington, Joseph R. (2013): An assessment of the suspended sediment rating curve approach for load estimation on the Rivers Bandon and Owenabue, Ireland. In *Geomorphology* 185, pp. 27–38. DOI: 10.1016/j.geomorph.2012.12.002.

Hoffmann, Carl Christian; Kjaergaard, Charlotte; Uusi-Kämppä, Jaana; Hansen, Hans Christian Bruun; Kronvang, Brian (2009): Phosphorus retention in riparian buffers: review of their efficiency. In *Journal of environmental quality* 38 (5), pp. 1942–1955. DOI: 10.2134/jeq2008.0087.

Horowitz, Arthur J. (2003): An evaluation of sediment rating curves for estimating suspended sediment concentrations for subsequent flux calculations. In *Hydrol. Process.* 17 (17), pp. 3387–3409. DOI: 10.1002/hyp.1299.

Horowitz, Arthur J. (2008): Determining annual suspended sediment and sediment-associated trace element and nutrient fluxes. In *The Science of the total environment* 400 (1-3), pp. 315–343. DOI: 10.1016/j.scitotenv.2008.04.022.

Horowitz, Arthur J.; Clarke, Robin T.; Merten, Gustavo Henrique (2015): The effects of sample scheduling and sample numbers on estimates of the annual fluxes of suspended sediment in fluvial systems. In *Hydrol. Process.* 29 (4), pp. 531–543. DOI: 10.1002/hyp.10172.

House, W. A.; Casey, H.; Donaldson, L.; Smith, S. (1985): FACTORS AFFECTING THE COPRECIPITATION OF INORGANIC PHOSPHATE WITH CALCITE IN HARDWATERS--I.

Ihringer; Liebert (2015): Abfluss-BW - regionalisierte Abfluss-Kennwerte Baden-Württemberg. Available online at https://www.lubw.baden-wuerttemberg.de/wasser/regionalisierte-abflusskennwerte, checked on 11/16/2018.

Institute for Water and River Basin Management, Department of Aquatic Environmental Engineering KIT (IWG-SWW) 2018: Supplementary Data. Provided by Adrian iwr (2018-10-10).

Khouja, Hamed (2000): Turbidimetry and Nephelometry, p. 1.

Kulasova, A.; Smith, P. J.; Beven, K. J.; Blazkova, S. D.; Hlavacek, J. (2012a): A method of computing uncertain nitrogen and phosphorus loads in a small stream from an agricultural catchment using continuous monitoring data. In *Journal of Hydrology* 458-459, pp. 1–8. DOI: 10.1016/j.jhydrol.2012.05.060.

Kulasova, A.; Smith, P. J.; Beven, K. J.; Blazkova, S. D.; Hlavacek, J. (2012b): A method of computing uncertain nitrogen and phosphorus loads in a small stream from an

agricultural catchment using continuous monitoring data. In *Journal of Hydrology* 458-459, pp. 1–8. DOI: 10.1016/j.jhydrol.2012.05.060.

Lake County Water Authority; USF Water Institute: Learn More About Trophic State Index (TSI) - Lake.WaterAtlas.org. Available online at http://www.lake.wateratlas.usf.edu/shared/learnmore.asp?toolsection=lm_tsi, checked on 11/6/2018.

Landwirtschaftliches Technologiezentrum Augustenberg (LTZA) (2018): P2O5-Oberbodengehalte für Acker- und Grünflächen auf Gemarkungsebene. Medianwerte der Jahre 1995-2012

Lannergård, Emma E.; Ledesma, José L. J.; Fölster, Jens; Futter, Martyn N. (2018): An evaluation of high frequency turbidity as a proxy for riverine total phosphorus concentrations. In *The Science of the total environment* 651 (Pt 1), pp. 103–113. DOI: 10.1016/j.scitotenv.2018.09.127.

Lawler, D.M (2014): Turbidity, Turbidimetry, and Nephelometry. In Jan Reedijk (Ed.): Reference module in chemistry, molecular sciences and chemical engineering. Oxford: Elsevier.

Lawler, D.M (Ed.) (2016): Reference Module in Chemistry, Molecular Sciences and Chemical Engineering: Elsevier.

LUBW (2018): Hochwasser-Vorhersage-Zentrale Baden-Württemberg: Frame-Set. Available online at https://hvz.lubw.baden-wuerttemberg.de/, updated on 1/25/2018, checked on 11/16/2018.

lva (2010): The EU Nitrates Directive-Water.

Mueller, D. K.; Helsel, D. R. (1999a): USGS NAWQA CIRC1136 Nutrients in Nation's Waters. Available online at https://pubs.usgs.gov/circ/circ1136/circ1136.html#INTRO, checked on 11/5/2018.

Mueller, D. K.; Helsel, D. R. (1999b): USGS NAWQA CIRC1136 Nutrients in Nation's Waters. Available online at https://pubs.usgs.gov/circ/circ1136/, checked on 11/5/2018.

Murphy, Sheila (2007a): BASIN: General Information on Nitrogen. Available online at http://bcn.boulder.co.us/basin/data/NEW/info/NH3.html, checked on 11/5/2018.

Murphy, Sheila (2007b): BASIN: General Information on Phosphorus (GeoPlanet: Earth and Planetary Sciences). Available online at http://bcn.boulder.co.us/basin/data/NEW/info/TP.html, checked on 11/4/2018.

Murphy, Sheila (2007c): BASIN: General Information on Total Suspended Solids. Available online at http://bcn.boulder.co.us/basin/data/NEW/info/TSS.html, checked on 11/5/2018.

Owens, P. N.; Batalla, R. J.; Collins, A. J.; Gomez, B.; Hicks, D. M.; Horowitz, A. J. et al. (2005): Fine-grained sediment in river systems: environmental significance and management issues. In *River Res. Applic.* 21 (7), pp. 693–717. DOI: 10.1002/rra.878.

Pollard, Peter (2013): UPDATED RECOMMENDATIONS ON PHOSPHORUS STANDARDS FOR RIVERS.

Quilbé, Renaud; Rousseau, Alain N.; Duchemin, Marc; Poulin, Annie; Gangbazo, Georges; Villeneuve, Jean-Pierre (2006): Selecting a calculation method to estimate sediment and nutrient loads in streams: Application to the Beaurivage River (Québec, Canada). In *Journal of Hydrology* 326 (1-4), pp. 295–310. DOI: 10.1016/j.jhydrol.2005.11.008.

Rajwa, Agnieszka; Bialik, Robert J.; Karpiński, Mikołaj; Luks, Bartłomiej (2014): Dissolved Oxygen in Rivers: Concepts and Measuring Techniques. In Robert Bialik, Mariusz Majdański, Mateusz Moskalik (Eds.): Achievements, History and Challenges in Geophysics. Cham: Springer International Publishing (GeoPlanet: Earth and Planetary Sciences), pp. 337–350.

Rekolainen, Seppo; Posch, Maximilian; Kämäri, Juha; Ekholm, Petri (1991): Evaluation of the accuracy and precision of annual phosphorus load estimates from two agricultural basins in Finland. In *Journal of Hydrology* 128 (1-4), pp. 237–255. DOI: 10.1016/0022-1694(91)90140-D.

Richard, Amy: Trophic State: A Waterbody's Ability To Support Plants, Fish, and Wildlife.

Rügner, Hermann; Schwientek, Marc; Egner, Marius; Grathwohl, Peter (2014): Monitoring of event-based mobilization of hydrophobic pollutants in rivers: calibration of turbidity as a proxy for particle facilitated transport in field and laboratory. In *The Science of the total environment* 490, pp. 191–198. DOI: 10.1016/j.scitotenv.2014.04.110.

Rymszewicz, A.; O'Sullivan, J. J.; Bruen, M.; Turner, J. N.; Lawler, D. M.; Conroy, E.; Kelly-Quinn, M. (2017): Measurement differences between turbidity instruments, and their implications for suspended sediment concentration and load calculations: A sensor inter-comparison study. In *Journal of environmental management* 199, pp. 99–108. DOI: 10.1016/j.jenvman.2017.05.017.

Sadeghi, S.H.R.; Mizuyama, T.; Miyata, S.; Gomi, T.; Kosugi, K.; Fukushima, T. et al. (2008): Development, evaluation and interpretation of sediment rating curves for a Japanese small mountainous reforested watershed. In *Geoderma* 144 (1-2), pp. 198–211. DOI: 10.1016/j.geoderma.2007.11.008.

Sara Bogialli; Stefano Polesello; Sara Valsecchi (2014): Quality Issues in Water Sampling, Sample Pre-Treatment and Monitoring.

Stevens, R. J.; Smith, R. V. (1978): A comparison of discrete and intensive sampling for measuring the loads of nitrogen and phosphorus in the river main, County Antrim. In *Water Research* 12 (10), pp. 823–830. DOI: 10.1016/0043-1354(78)90033-7.

The German Advisory Council on the Environment (2015): The implementation of the Water Framework Directive in Germany with regard to nitrogen inputs from agriculture.

US EPA: 4. What are EPA's drinking water regulations for nitrite? Edited by 1992. Available online at https://safewater.zendesk.com/hc/en-us/articles/211401678-4-What-are-EPA-s-drinking-water-regulations-for-nitrite-, checked on 11/5/2018.

US EPA (1998): 1998 National Nutrient Strategy, p. 44.

US EPA (2003): DEVELOPING WATER QUALITY CRITERIA FOR SUSPENDED AND BEDDED SEDIMENTS (SABS).

Vercruysse, Kim; Grabowski, Robert C.; Rickson, R. J. (2017): Suspended sediment transport dynamics in rivers: Multi-scale drivers of temporal variation. In *Earth-Science Reviews* 166, pp. 38–52. DOI: 10.1016/j.earscirev.2016.12.016.

Voichick, Nicholas; Topping, David J.; Griffiths, Ronald E. (2018): Technical note: False low turbidity readings from optical probes during high suspended-sediment concentrations. In *Hydrol. Earth Syst. Sci.* 22 (3), pp. 1767–1773. DOI: 10.5194/hess-22-1767-2018.

Walling, D. E. (2006): Human impact on land–ocean sediment transfer by the world's rivers. In *Geomorphology* 79 (3-4), pp. 192–216. DOI: 10.1016/j.geomorph.2006.06.019.

Wikipedia (Ed.) (2018): Kraichbach - Wikipedia. Available online at https://en.wikipedia.org/w/index.php?oldid=837029110, updated on 9/30/2018, checked on 10/1/2018.

Yang, Chi-Cheng; Lee, Kwan Tun (2018): Analysis of flow-sediment rating curve hysteresis based on flow and sediment travel time estimations. In *International Journal of Sediment Research* 33 (2), pp. 171–182. DOI: 10.1016/j.ijsrc.2017.10.003.